Dalton Transactions

Accepted Manuscript

This article can be cited before page numbers have been issued, to do this please use: F. D. Pammer, J. D. W. Schepper, J. Glöckler, Y. Sun and A. Orthaber, *Dalton Trans.*, 2019, DOI: 10.1039/C9DT01555H.

ROYAL SOCIETY OF CHEMISTRY

rsc.li/dalton

ROYAL SOCIETY OF CHEMISTRY View Article Online
DOI: 10.1039/C9DT01555H

Journal Name

ARTICLE

Expansion of the scope of alkylboryl-bridged N→B-Ladder boranes: New Substituents and alternative substrates

Received 00th January 20xx,
Accepted 00th January 20xx

DOI: 10.1039/x0xx00000x

www.rsc.org/

Frank Pammer,*[a†] Jonas Schepper,[a†] Johannes Glöckler,[b†] Yu Sun,[c] Andreas Orthaber[d].

A series of new boranes capable of forming intramolecular N→B-heterocycles has been prepared and their properties have been studied by electrochemical methods and UV-vis-spectroscopy complemented by DFT calculations. A dimethylborane (**BMe$_2$**), haloborane derivatives (**BBr$_2$**, **BF$_2$**, **BI$_2$**) and mixed cyano/isocyano-borane (**B(CN)(NC)**) have been prepared by different techniques. Furthermore, 2'-alkynyl-substituted 2-phenylpyridines bearing terminal *tert*-butyl- and trimethylsilyl-groups are introduced as a new class of substrates for hydroboration. Successful hydroboration with either 9*H*-borabicyclo[3.3.1]-nonane (9*H*-BBN), dimesitylborane (Mes_2B-H), or Piers' borane ($(C_6F_5)_2$B-H, BPF-H) furnished new π-extended boranes capable of forming intramolecular six- or seven-membered N→B-heterocycles (***t*BuBBN**, **SiBPF**), and, in the case of Mes_2BH, formation of a sterically crowded styrylborane (**SiBMes$_2$**) incapable of intramolecular N→B-coordination was observed. All boranes listed above except **BMe$_2$** have been structurally characterized, and a study of their electrochemical properties showed that the systematic variation of the substituents on boron allows for the incremental variation of the electron affinity of the phenylpyridine-model system over a total range of > 0.7 eV between alkylboranes (**BMe$_2$**, **BBN**) and **B(CN)(NC)**. **B(CN)(NC)** shows the strongest N→B-bond (≈ 175 kJ/mol), and highest electron-affinity observed so far, and is the first example of a borane bearing an isocyano-substituent on boron.

Introduction

Boron containing conjugated organic materials have attracted the interest of synthetic chemists for years and new potential applications for these compounds continuously emerge.[1] The tailoring of the electronic properties of π-conjugated organic materials through incorporation of boron, has been widely employed to tailor their optical and electronic properties. Either through attachment of boryl-groups to conjugated systems,[2,3] or in the form of tetracoordinate boron centers bearing *N,O*^{2}-*N,N*^{2}-chelating ligands, i.e. ladder compounds.[4] What renders ladder boranes so interesting, is their potential use in organic light emitting devices,[4,5] and the recent finding, that ladder-polymers containing intramolecular N→B-coordinated bridging units can serve as electron acceptors in organic photovoltaic cells.[6] This paper is concerned with ladder boranes featuring *N,C*^{2}-chelated ladder boranes, which have been investigated to much lesser degree than other molecular architectures. However, since being first introduced by Yamaguchi (**A**, Chart 1), *N,C*^{2}-chelated ladder boranes may have been discussed as potential electron-transporting (n-type) materials,[7] and have since been successfully employed as n-channel organic field effect transistors,[8] and as donors in organic photovoltaics that provide an increased cell voltage (**B**, Chart 1).[9]

The most widely used methods to prepare N→B-ladder boranes is direct electrophilic C-H-borylation with boron halides,[10] which can even serve to post-functionalize polymers,[11] or the step-wise metalation and electrophilic borylation of suitable precursors.[12] Other methods involve intramolecular nucleophilic aromatic substitution,[13] 1,3-dipolar azide-alkyne cycloaddition,[14] and unusual 1,1-hydroboration of benzoisoindoles.[15] The latter method[15] furnishes alkyl-boryl bridged ladder boranes (**C**, Chart 1). This sub-class of ladder-boranes is of particular interest, because they can be converted into fully conjugated *B,N*-doped condensed arenes (**D**, Chart 1), either thermally, photochemically,[16] or within a working light emitting device.[5]

[a] Dr. F. Pammer, M. Sc. Jonas Schepper
Institute of Organic Chemistry II and Advanced Materials
University of Ulm
Albert-Einstein-Allee 11, 89081 Ulm, Germany
E-mail: frank.pammer@uni-ulm.de
[b] M. Sc. Johannes Glöckler
Institut of Analytical and Bioanalytical Chemistry
University of Ulm
Albert-Einstein-Allee 11, 89081 Ulm, Germany
E-mail: johannes.gloeckler@uni-ulm.de
[c] Dr. Y. Sun
Fachbereich Chemie
Technische Universität Kaiserslautern
Erwin-Schrödinger-Strasse 54, D-67663 Kaiserslautern, Germany
E-mail: sun@chemie.uni-kl.de
[d] A. Orthaber,
Department of Chemistry – Ångström laboratories
Uppsala University
BOX 523, 75120 Uppsala, Sweden
E-mail: andreas.orthaber@kemi.uu.se

† Authors contributed equally
Supporting information for this article available on the www under http//dx.doi.org/10.1002/.XXXXXXXXXX.

View Article Online
DOI: 10.1039/C9DT01555H

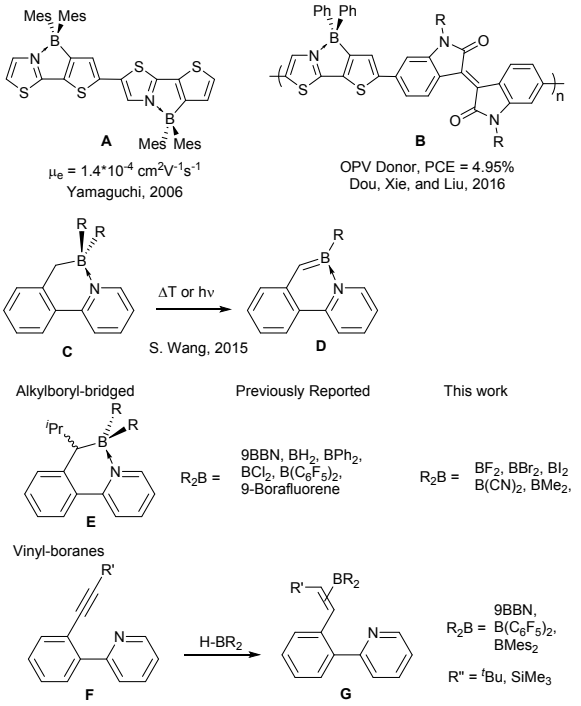

Chart 1. Previously reported alkylboryl-bridged boranes, and new boranes reported herein. See Scheme 1 for details on compounds of type **E**.

In our group, we explored the scope of the preparation of alkylboryl-bridged N→B-ladder-boranes by hydroboration of suitable substrates. We could demonstrate, that this approach allows to convert a variety of *N*-heterocyclic substrates in high yield,[17,18,19] serves to introduce a whole range of boryl-substituents (**E**, Chart 1),[20] and is also suitable for the post-functionalization of polymers.[21,22]

In this paper, we report our latest efforts to broaden the scope of this preparative strategy (**E**, Chart 1), and report a series of new vinylborane-containing N→B-ladders (**G**, Chart 1) generated by hydroboration of alkynes (**F**, Chart 1).

Results and Discussion

Alkylboryl-bridged Ladder-Boranes

Synthesis and Structures: In order to expand our survey of the effect of substituents on boron on the properties of the conjugated π-system in N→B-ladder boranes, we endeavored to expand the series of previously known derivatives (**Scheme 1**).

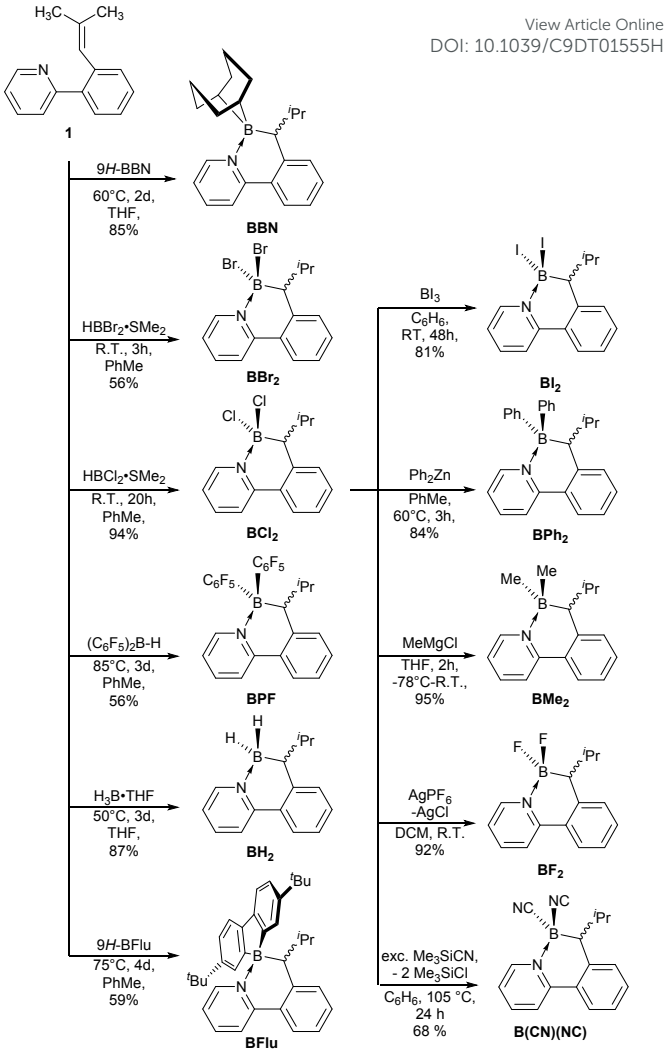

Scheme 1. Synthesis of alkylboryl-bridged boranes. **BF$_2$**, **BBr$_2$**, **BI$_2$**, **BMe$_2$**, and **B(CN)(NC)** newly reported herein. All other compounds previously included in Ref. 20.

Firstly, we set out to complete the series of dihaloboranes. Among these, the dibromoboryl-derivative **BBr$_2$** is directly accessible in 56% yield by hydroboration of the *ortho*-styryl-pyridine substrate (**1**) with commercially available Br$_2$BH•SMe$_2$. Other derivatives can be prepared from the previously reported **BCl$_2$**. The diiodo-derivative was obtained in good yield (81%) by treatment of **BCl$_2$** with an excess of boron triiodide (BI$_3$), which leads to its full conversion into **BI$_2$** within minutes. In a serendipitous finding, **BF$_2$** was formed in near quantitative yield (92%) upon treatment of **BCl$_2$** with one equivalent of silver(I) hexafluorophosphate. Evidently, the borenium cation formed upon abstraction of chloride, rapidly abstracts fluoride from the PF$_6$-counter anion. Importantly, this reagent proved much more effective than the use of silver(I) fluoride, which provided only 67% yield, even when employed in excess. Furthermore, reaction of **BCl$_2$** with MeMgCl gave **BMe$_2$** in excellent yield. The above compounds were fully characterized by ^{1}H, ^{13}C, and ^{11}B NMR, and all except **BMe$_2$** could also be unambiguously identified by single crystal X-ray crystallography (vide infra).

The chemical shifts in the ^{11}B NMR range from +6.7 ppm (C$_6$D$_6$, all data recorded in C$_6$D$_6$, unless stated otherwise) for **BF$_2$**, and

+4.9 ppm for **BBr_2** to -2.4 and -12.6 ppm for **BMe_2** and **BI_2**, respectively. These values are in the expected range for tetra-coordinate boron, and indicate, that N→B-coordination persists in solution. The observed sequence of chemical shifts for the dihalo-boranes is also in agreement with previous reports on base adducts of dihalo-alkylboranes ($R_3N→R'BI_2$: -17.5 ppm,[23] $R_3N→MeBBr_2$: +6.4 ppm,[24] $Et_3N→EtBF_2$: +6.7 ppm[25]). **BF_2** and **BMe_2** can also be identified by the respective NMR signals of their diastereotopic substituents on boron. **BF_2** shows two broadened signals in the ^{19}F NMR spectrum at -148.0 ppm and -162.1 ppm (in C_6D_6), while the ^1H NMR signals of the BMe_2-group in **BMe_2** are observed as broadened singlets at 0.61 and 0.15 ppm (C_6D_6).

With this series of compounds, we have completed the full series of homologous haloboranes. Significantly, to the best of our knowledge, this is only the second report of a diiodo-alkylborane.[23] The development of a preparative access to this compound constitute a significant finding, since **BI_2** may serve as a versatile starting material for further organometallic transformations.

A highly unusual find was made in an attempt to further extend the spectrochemical series: Prolonged heating of **BCl_2** in benzene in the presence of an excess of Me_3Si-CN[26] resulted in the clean conversion of the starting material. Monitoring of the reaction by ^1H NMR (see Figure S29 in the ESI) shows the stepwise consumption of **BCl_2**, and the concurrent formation of two intermediates, which we presume to be the diastereomeres of the mono-substitution product (**B(CN)Cl**). The intermediates are eventually consumed, and a final single product is formed that was deemed to be the dicyano derivative **BCN_2**. However, IR-spectroscopy and analysis of single crystals by X-ray diffraction revealed, that instead of the dicyano-borane, a mixed borane is formed that contains one cyano- and one isocyano ligand. The compound will therefore in the following be referred to as **B(CN)(NC)**. IR spectra show two characteristic bands of comparable strengths at $\tilde{\nu}$ = 2211 and 2125 cm^{-1}, that can be attributed to the stretching vibration of isocyano- (B-N≡C) and cyano-moiety (B-C≡N), respectively.[27] The cyano carbon atom could not be observed by ^{13}C NMR at a chemical shift in the expected range at δ = XXXX ppm.[30] Still, the isocyano-group could not be directly observed, due to the low intrinsic receptivity this type of carbon atoms. Similarly, variable ^1H NMR spectra down to -80°C show only a single set of signals (see Figure S30 in the ESI), even though the diastereomeres of **B(CN)(NC)** should be just as readily distinguishable, as those of the presumed **B(CN)Cl** intermediate. It is therefore not absolutely certain at this point, whether the **B(CN)(NC)**-structure is merely present in the solid state, or also persists in solution. The resonance in the ^{11}B NMR spectrum observed at -13.0 ppm is in agreement with the N→B-coordination persisting in solution.

Furthermore, quantum chemical calculations (vide infra) also indicate that the coordinative bond to the pyridyl nitrogen (≈ 175 kJ/mol) is among the strongest encountered so far for any of the alkylboryl-bridged ladder boranes discussed herein. It is therefore likely, that the coordination of the (iso)cyano-ligands is not labile.

Borate anions featuring isocyano- groups have been reported previously,[28] as well as neutral nitrogen-base adducts of isocyanoboranes.[29] While anionic isocyanoborates can be isolated,[30] and employed as anionic ligands to transition metals,[31,32] the neutral boranes rather exist as dynamic mixtures and isomerize to the isocyanide-coordination mode in the presence of suitable metal centers.[33,34,35] To the best of our knowledge, this is therefore the first example of a stable neutral isocyanoborane that can be isolated in substance.

Single crystals of **B(CN)(NC)** for analysis by X-ray diffraction where obtained by layering the reaction mixture with hexane (Figure 1 D). **B(CN)(NC)** crystalizes in the monoclinic space group $P12_1/c1$ with four molecules in the unit cell, and adopts an N→B-coordinated structure in the solid state. Analogous to previously described *ortho*-styryl-azine derived ladder boranes,[17,18,19] the isopropyl groups adopts an axial orientation in the central six-membered N→B-ring. Consequently, one substituent on boron is oriented in a *trans*-axial position relative to the ^{i}Pr-group, while the other adopts an equatorial orientation. The crystal structure unambiguously confirmed the presence of the isocyano-ligand, although the substituents on

Table 1. Space groups, characteristic bond lengths [Å] and angles [°] of the synthesized ladder compounds derived from their crystal structures, and structural parameters calculated by DFT. Numbering according to Figure 2. C_{iPr}: methin-*C* of axial *i*Pr-group. X_{ax}: axial substituent on boron.

Borane	Space Group	N1→B1	N1-C5-C6-C11	C5–C6	C12–B1	CiPr-C12-B1-X_{ax}	C5-N1-B1-X_{ax}	DFT[b] N→B / N1-C5-C6-C11		^{11}B NMR[c]
		[Å]	[°]	[Å]	[Å]	[°]	[°]	[Å]	[°]	[ppm]
BF_2	P-1	1.589(3)	18.1(2)	1.485(3)	1.591(3)	162.2(1)	86.6(2)	1.664	20.3	+6.7
BCl_2[a]	P21/c	1.596(4)	19.6(3)	1.483(4)	1.592(4)	166.2(1)	84.4(2)	1.623	22.5	+9.4
BBr_2	$P4_2/n$	1.588(3)	18.5(3)	1.482(3)	1.591(3)	170.1(1)	75.0(2)	1.614	22.2	+4.9
BI_2	$P12_1/c1$	1.579(6)	-22.4(6)	1.473(6)	1.598(6)	168.0(3)	-86.7(3)	1.594	22.9	-12.6
B(CN)(NC)	$P12_1/c1$	1.592(2)	23.6(2)	1.475(2)	1.613(2)	167.9(7) (C) 169.3(7) (N)	85.4(7) (C) 81.7(7) (N)	1.626	22.7	-13.0

[a] Included for reference purposes. Data adopted from Ref. 20. [b] From ^{i}Pr$_{ax}$-structures optimized by DFT at the M06-2X/6-31G(d,p) level of theory. [c] Recorded in C_6D_6.

the boron atom were systematically disordered. The crystallographic data for **B(CN)(NC)** is in best agreement with the presence of one cyano- and one isocyano-ligand in either axial or equatorial position, with a preference (60%) of the isocyano-ligand to be located in an axial orientation.

The coordinative N→B-bond to the pyridine ring measures 1.592(2) Å, and is therefore the shortest yet observed for this type of ladder borane, except for the three newly reported haloboranes: **BF_2**, **BBr_2**, and **BI_2** crystallize in the space-groups P-1 (Z=2, triclinic), P42/n (Z=8, tetragonal), and $P12_1/c1$ (Z=4, monoclinic), respectively. Similar to **B(CN)(NC)** and previously described ladder boranes,[17,18,19] the isopropyl groups in all three compounds also adopt an axial orientation in the central six-membered N→B-ring. The N→B-bond lengths range from d(N→B) = 1.589(3) Å for **BF_2**, and d(N→B) = 1.588(3) Å for **BBr_2**, to d(N→B) = 1.579(6) Å for **BI_2**. The coordination is therefore tighter than in **BCl_2** (d(N→B) = 1.596(4) Å)[17] and **BH_2** (d(N→B) = 1609(2) Å).[17] This sequence does not quite reflect the typically observed order of Lewis acidity of haloboranes (BI_3>BBr_3>BCl_3>BH_3>BF_3).[36] Particularly the less tight coordination in **BCl_2** and the short N→B-coordination in **BF_2** are surprising. This observation may be attributable to a combination of steric and electronic factors, since boron-halogen-bonds to axial halogens are generally longer than to equatorial halogens. The steric contributions are apparent from the fact that effect is negligible for **BF_2** (Δd(B-F)ax/eq = 0.003 Å), and substantially larger for **BCl_2**, **BBr_2**, and **BI_2** (Δd(B-X)ax/eq = 0.033-0.028 Å).

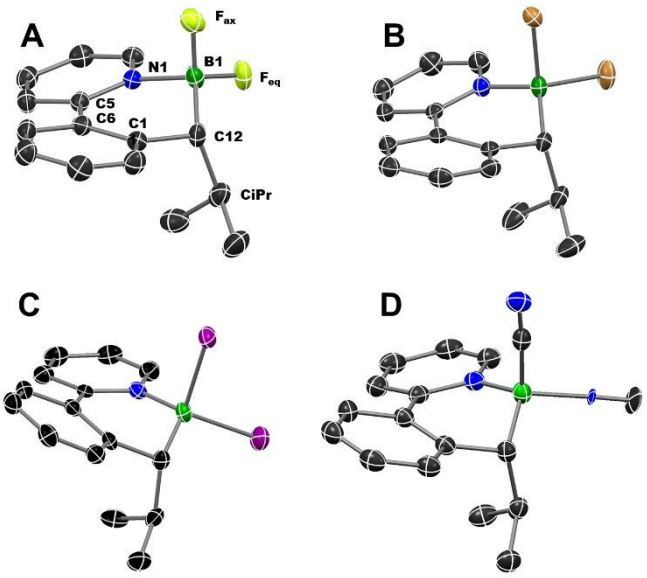

Figure 1. A: Crystal structures of N→B-ladder boranes. **A: BF_2**; **B: BBr_2**; **C: BI_2**; **D: B(CN)(NC)**. Structures shown at 55% probability level. Hydrogen atoms have been omitted for clarity. Representative labels shown for **BF_2** in **A**.

Optical and electrochemical properties: Analyses of the phenylpyridine-derived ladder boranes by UV-vis spectroscopy showed comparable absorption spectra in all cases, with longest-wavelength absorption maxima (λ_{max}) between 304 (**BMe_2**) and 316 nm (**BBr_2**). Also present in the absorption spectra are underlying absorption bands at longer wave-lengths that give rise to clearly visible shoulder bands in the spectra of **BMe_2** and **BBr_2**, while a shoulder band in the spectrum of **BF_2** is somewhat less pronounced. Simulation of UV-vis spectra by time-dependent DFT (TDDFT) calculations showed that these underlying bands are most likely attributable to absorption of N→B-coordinated conformers, wherein the isopropyl-group assumes an equatorial conformation, instead of the energetically favorable axial conformation (*vide infra*).

The **BI_2** derivative shows a λ_{max} (305 nm) in the same range as the other halo-boranes. However, the absorption only gradually fades towards longer wave-length and reaches the baseline at approximately 400 nm (see Figure 2B and Figure S4 in the ESI). Initially, we attributed this latter observation to inadvertently decomposition of **BI_2**. However, TD-DFT calculations indicate that the red-shifted absorption onset may be attributed to very weakly populated n-to-π*-transitions from lone-pairs on the iodide-ligands to π*-orbitals delocalized across the phenyl-pyridine ring-system (*vide infra*).

The influence of the substituents on boron was further elucidated through investigation of the electrochemical reduction potentials by square-wave voltammetry (SWV) and cyclic voltammetry (CV, all potentials reported in the following have been referenced vs. FcH/FcH^+, peak potential E_p have been determined by SWV). All new boranes except **BF_2** exhibited only irreversible reduction waves in CV experiments (see Figure S1 in the ESI for details). However, the results of the SWV measurements (**Figure 2A**), allowed for a reliable comparison of these results with data for previously reported compounds. The reduction peak of **BMe_2** appeared broadened, but agrees well with the one of **BBN**. As expected, these diakylboranes therefore exhibit very similar electron affinities. Among the new boranes only **BF_2** underwent reversible electrochemical reduction (see Figure S1 in the ESI), and also showed the lowest electron affinity of all haloboranes with a peak current at E_{peak}^{red} = -2.26 V (SWV) relative to the ferrocene/ferrocenium redox couple. This value lies right between those of the previously reported bisphenyl- and bis(pentafluorophenyl)-derivatives **BPh_2** (E_p^{red} = -2.40 V, and **BPF** (E_p^{red} = -2.20 V), and therefore closed a rather large gap in this series. Reduction of **BBr_2** occurred close to the potential as observed for **BCl_2** at E_p^{red} = -2.05 V. However, this compound was less "well-behaved" and gave more broadened signals, presumably due to decomposition of the reduced species. Similarly, no reliable electrochemical data could be obtained for **BI_2**. A surprising find turned out to be **B(CN)(NC)**, which exhibited the highest electron-affinity in this series. Although this borane exhibited only irreversible reduction (see Figure S1 in the ESI), a sharp peak current was observed in SWV experiments at E_{peak}^{red} = -1.95 V. This finding indicates that dicyanoboryl-ladder may exhibit much higher electron affinities and higher redox-stability than haloboranes.

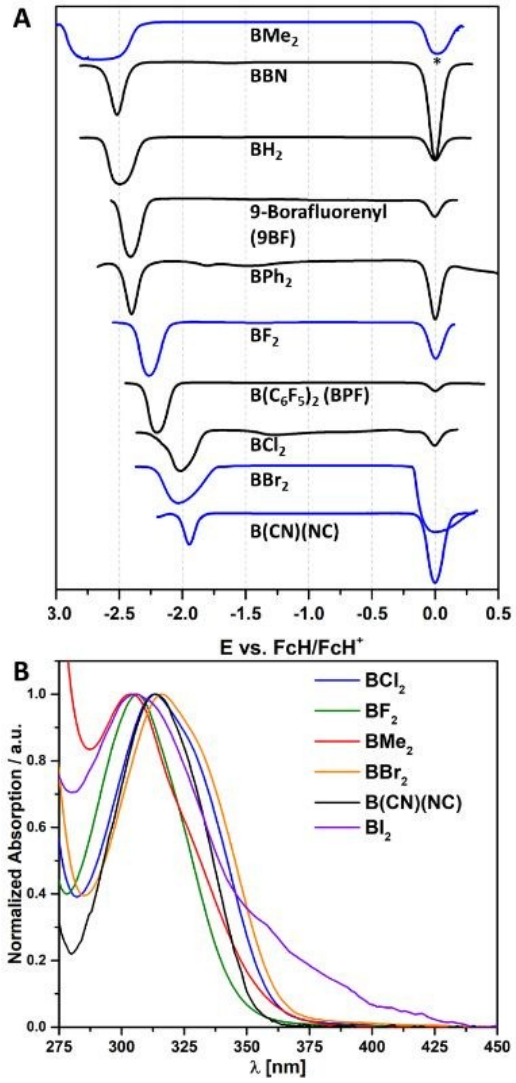

Figure 2. A: Square-wave voltammetry scans of new N→B-ladder boranes (blue) and previously reported boranes (black). Recorded in THF with 0.1M NBu_4PF_6 as supporting electrolyte at a scan rate of 200 mV/s. * internal standard Ferrocene. **B:** UV-vis Absorption spectra of new boranes in THF-solution. **BCl_2** included for reference.

DFT-calculations: To compare the properties of the new compounds with previously reported ladder boranes, and to elucidate the origin of their optical properties, the new boranes were simulated by quantum chemical simulations. Geometry optimizations at the M06-2X/6-31G(d,p) level of theory were performed for three conformers of each borane: two N→B-coordinated ones with the isopropyl-group placed either in an *equatorial* (***i*Pr$_{eq}$**) or an *axial* (***i*Pr$_{ax}$**) position, as well as an ***open*** (**open**) conformer without N→B-bond (**Table 2**). In the case of the cyano-substituted borane the survey was expanded: ***i*Pr$_{eq}$**- and ***i*Pr$_{ax}$**-, and ***open***-conformers of the dicyano-borane (**B(CN)$_2$**), the diisocyanoborane (**B(NC)$_2$**), and **B(CN)(NC)**-derivatives bearing the isocyano-substituent either in an axial (**B(CN)(NC$_{ax}$)**) or in an equatorial (**B(CN)(NC$_{eq}$)**) orientation were simulated.

Table 2. Schematic representation of possible borane conformers and calculated relative energies in kJ/mol.

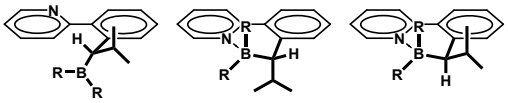

	open	*i*Pr$_{ax}$	*i*Pr$_{eq}$
BMe$_2$	+83	0	+12
BF$_2$	+91	0	+11
BCl$_2$	+120	0	+10
BBr$_2$	+135	0	+11
BI$_2$	+124	0	+8
B(CN)(NC$_{ax}$)[a]	+177	+23	+36
B(CN)(NC$_{eq}$)[a]	+177	+23	+33
B(CN)$_2$	+176	:= 0[a]	+14
B(NC)$_2$[a]	+179	+40	+51

[a] Data for **B(NC)$_2$**, **B(CN)(NC$_{ax}$)**, and **B(CN)(NC$_{eq}$)** given relative to ***i*Pr$_{ax}$**-conformer of **B(CN)$_2$**.

In agreement with previous findings, ***i*Pr$_{ax}$** conformers are generally the most favorable (**Table 2**). However, the corresponding ***i*Pr$_{eq}$** conformers are only between 8 (**BI$_2$**) and 13 kJ/mol (**B(CN)(NC$_{ax}$)**) higher in energy, and should therefore be thermally populated. ***Open*** conformers are between 83 kJ/mol (**BMe$_2$**) and 135 kJ/mol (**BBr$_2$**) higher in energy. Notably, **BF$_2$** shows the weakest N→B-coordination (ΔE = 91 kJ/mol) among the haloboranes, while the N→B-bond is strongest in **BBr$_2$**. The strongest yet observed N→B-bonds were found for cyano-substituted boranes, with decoordinated conformers being between +176 kJ/mol and +179 kJ/mol higher in energy than the ***i*Pr$_{ax}$** conformer of **B(CN)$_2$** - the most stable isomer (:= 0 kJ/mol). The diisocyano-derivative **B(NC)$_2$** is the least stable one (+40 kJ/mol for ***i*Pr$_{ax}$**, +51 kJ/mol for ***i*Pr$_{eq}$**), while the experimentally observed derivatives **B(CN)(NC$_{ax}$)** and **B(CN)(NC$_{eq}$)** lie between the two (+23 kJ/mol).

The optical properties of the boranes were also computed by time-dependent DFT (TDDFT) calculations for ***i*Pr$_{ax}$**, ***i*Pr$_{eq}$**, and ***open*** conformers (see Figure S4 in the ESI), and UV-vis absorption spectra were simulated. Analyses of the involved optical transitions revealed, that for all N→B-coordinated boranes, the lowest energy transitions are near exclusively HOMO-to-LUMO in character (see Section 2 of the ESI for listed data, and Orbital plots). While the LUMOs are typically π*-orbitals delocalized across the phenyl-pyridine backbone, the exact nature of HOMO-orbitals varies: For **BF$_2$** the HOMO is a π-orbital delocalized throughout the phenyl-pyridine, while the HOMO of **BMe$_2$** also shows σ-type contributions from electron rich B-CH_3 bonds. In contrast, the HOMOs of **BBr$_2$** and particularly **BI$_2$** are increasingly dominated by contribution from the lone-lairs on the halogen atoms. ***Open*** conformers show more complex lowest energy transitions, since the LUMO is dominated by the p_z-orbital on boron, which is not conjugated to the π-system. As a consequence, optical transitions of ***open*** conformers are expected to occur at much shorter wavelength

View Article Online
DOI: 10.1039/C9DT01555H

than those of N→B-coordinated conformers. Furthermore, a common feature observed for the N→B-ladder conformers of **BF_2** and **BBr_2** and **BMe_2** is that the ***i*Pr$_{eq}$**-conformers – which are higher in energy, but can be thermally populated - exhibit lowest energy transitions that are between 0.31 and 0.25 eV lower in energy than those of the corresponding ***i*Pr$_{ax}$**-conformers. A qualitative comparison of the simulated UV-vis spectra with the experimental data indicates that the longer wavelength shoulder bands in the absorption spectra of these compounds originate from a superimposition of the absorption of both conformers.

Furthermore, analysis of the expected absorption features of **BI_2** showed, that this borane would be expected to show a much red-shifted absorption. The lowest energy transition is calculated at 3.17 eV (f = 0.003) for the ***i*Pr$_{ax}$** -derivative (***i*Pr$_{eq}$** : 3.33 eV, f = 0.004), and is therefore at least 0.7 eV lower in energy than in any other borane investigated in this survey. The reason for their weak population is that they represent formally forbidden n-to-π*-transitions from lone-pairs on iodide atoms to π*-type LUMO on the phenyl-pyridine system. These low intensity transitions explain the only gradual fading of the optical absorption, and therefore clarify, that the experimental data indeed originated from the **BI_2**, rather than from inadvertent decomposition products.

The electronic situation in **B(CN)(NC)** is very similar to e.g. **BF_2** with the exception that for ***open*** conformers of this compounds much lower energy longest-wavelengths absorptions would be expected, that are in the same range as for the N→B-coordinated conformers. However, since the N→B-bond in this compound is the strongest of all included in this survey, we still attribute the observed absorption features to the ladderized conformers. ***i*Pr$_{eq}$** conformers again show longer-wavelength absorption, and optical transitions remain almost unaffected by switching isocyano-substituent from an axial to an equatorial position. The weak shoulder band in the experimental absorption spectrum of **B(CN)(NC)** is therefore also assigned to a superimposition of the absorption of ***i*Pr$_{eq}$** and ***i*Pr$_{ax}$** conformers.

Summarizing the results discussed above, we have successfully expanded the range of accessible N→B-ladder boranes across the whole range of haloboranes, and also made a pseudo-halide derivative (**B(CN)(NC)**) available, that shows the strongest N→B-bond, and highest electron-affinity yet. These results are fully consistent with our previous reports, and therefore significantly expand the knowledge base to further explore this chemistry.

Preparation and Properties of Vinylboranes

Synthesis and structure: A key drawback of the above strategy was, that the resulting N→B-ladder-boranes cannot be converted into fully conjugated B-N-isosters, unlike methylene-boryl-bridged boranes (Chart 1, **C**).[5] We therefore considered the mono-hydroboration of alkynes as an alternative strategy to generate the corresponding vinylboranes (**B4**, **Scheme 2Figure 3**). These might then be isomerized into the corresponding *B,N*-isosters featuring tricoordinate boron (**B3**).

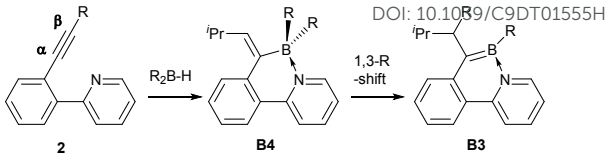

Scheme 2. Generation of vinyl-borane-containing N→B-ladders and their conversion into *B,N*-isosters.

Wang and co-workers recently showed that hydroboration of 2-alkynyl-pyridines yields vinylboranes that form intramolecularly N→B-coordinated five-membered rings via a formal *trans*-hydroboration.[37] Curiously, while hydroboration of 2-ethynylpyridine[38,37] results in exclusive borylation at the α-position, in the above case borylation of the internal triple bond favored the β-position. This latter selectivity would not allow for the desired intramolecular N→B-coordination, as indicated in **Scheme 2**. We therefore experimentally explored the hydroboration of two substrates equipped with more sterically demanding *tert*-butylethynyl- (**2a**, R = ^{t}Bu)[39] and trimethylsilylethynyl-side chains (**2b**, R = $SiMe_3$), to enforce the desired α-borylation. While hydroboration of terminal alkynes readily proceeds at ambient temperature, hydroboration of the present substrates required more forcing conditions, simple mixing of the reagents just resulted in adduct formation.[40] Nevertheless, prolonged heating of **2a** in the presence of 9*H*-BBN resulted in conversion of the substrate alkyne and allowed isolation of the α-vinyl-borane ***tBu*BBN** in 43% yield. The steric pressure of the *tert*-butyl group enforced borylation in the benzylic position, and even though the ***t*BuBBN** is still highly strained, it is still capable of forming an intramolecular N→B-bond in solution, as indicated by ^{11}B NMR signals at 0.0 ppm in C_6D_6 and -2.7 ppm in THF-d_8. However, simulations of ***open*** and ***closed*** structures indicate that the N→B-coordinated conformer is only 45 kJ/mol lower in energy. The N→B-coordination is therefore weaker than in any of the previously investigated systems. For instance, the N→B-bond in the styrylpyridine derived analogue[41] was estimated to be about 69 kJ/mol strong.[17] After this exploratory experiment, we further investigated the hydroboration of **2b** (R = $SiMe_3$). The Me_3Si-group was meant to serve as a protecting group that may eventually be removed to access an unsubstituted borane. In contrast to the previous results, hydroboration with 9*H*-BBN resulted in unspecific decomposition of the substrate, and did not allow the isolation of a product. Surprisingly, hydroboration was possible with dimesitylborane (Mes_2BH[42]), and the product **$SiBMes_2$** was isolated in 32% yield. Notably, analysis by X-ray crystallography showed that **$SiBMes_2$** is borylated at the β-position, despite the resulting steric hindrance. While this result can be explained by the well-known β-silicon effect,[43,44,45] the geminal borylation of the highly sterically encumbered borane and the TMS groups is still surprising. Furthermore, due to the *syn*-addition of Boron and hydrogen **$SiBMes_2$** cannot form an intramolecular N→B-bond. In a final experiment, the borylation was performed using Piers' Borane ($(C_6F_5)_2BH$, BPF-H[46]), which again allowed the isolation of a well-defined product (**SiBPF**) in 40% yield. The reaction again results in silicon-directed

borylation at the β-position. However, 1,2-hydroboration and formation of the BPF-analogue to **SiBMes$_2$**, does not occur. Instead, under the reaction conditions, the TMS-group migrates to the benzylic α-atom and thus furnishes the formal 1,1-hydroboration product **SiBPF**. Notably, the highly Lewis-acidic vinyl-B(C_6F_5)$_2$-group can still coordinate onto the pyridyl-nitrogen under formation of a seven-membered 1,2-azaborepine-ring. Furthermore, the N→B-bond evidently persists in solution, since **SiBPF** shows a signal in the ^{11}B NMR at -4.7 ppm. According to DFT-calculations, the strength of the N→B-bond is about 90 kJ/mol, and therefore ca. 30% weaker than the N→B-coordination in the analogous styrylpyridine-derived BPF-containing phenyl-pyridine (≈132 kJ/mol[17]).

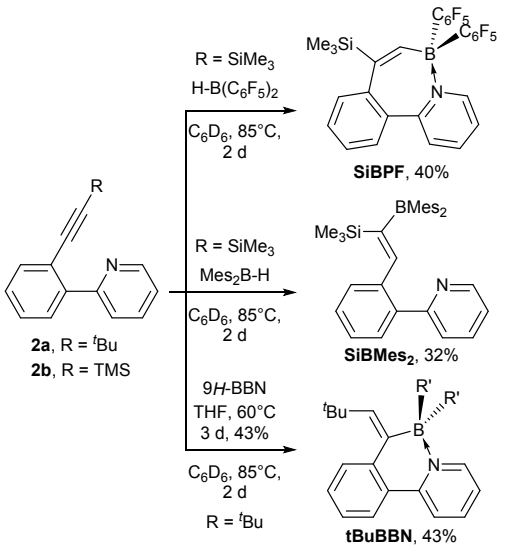

Scheme 3. Preparation of vinylboranes by hydroboration.

The three vinyl-boranes could be crystallized and were analyzed by single-crystal X-ray crystallography. For ***t*BuBBN** the crystal structure reveals an N→B-coordinated conformation in the solid state. With a bond-length of 1.662(4) Å, the coordinative bond is weakened compared to its styrylpyridine-derived analogue (1.646(2) Å[17]). Still, coordination is tighter than in more sterically encumbered boranes,[17] or systems with less Lewis-basic *N*-heterocycles.[14,17] The central N→B-heterocycle assumes a half-chair conformation, with a biaryl-torsion of 25.8(4)°. To allow for this torsion, the *tert*-butyl-vinyl-group has to bend out of the ring-plane, which result in an angle between the phenyl-ring-plane and the vinylic C=C-bond of 51.5(1)°. The crystal structure of **SiBMes$_2$** confirms the β-borylation, and the presence of a tricoordinate dimesityl-vinyl-borane. The steric pressure of the TMS-group does not directly affect the boryl group. The bond between boron and the vinylic carbon atom (d(B1-C12) = 1.563(3) Å), and the adjacent C=C-double bond (d(C12-C13) = 1.354(2) Å) are within the typical range for the kind of system (e.g. *n*C_5H_{11}-C(BMes_2)=CH-thienyl[47]: B-C_{vinyl} = 1.565(8) Å, C=C = 1.350(7) Å, C=C-C_{Ar}-C_{Ar} = 37.1(8)°). Still, compared to this reference system, the additional steric pressure from the TMS-groups leads to a stronger torsion between the vinyl-group and the aryl-system (**SiBMes$_2$**: C=C-C_{Ar}-C_{Ar} = 53.4(2) Å).

Analysis of the solid-state structure of **SiBPF** confirmed the formation of a seven-membered N→B-heterocycle. The ring adopts a boat-conformation with the tetracoordinate boron center located at the 'bow'. The N→B-coordination (**SiBPF**: d(N→B) = 1.640(2) Å) is less tight than in the BPF-containing styrylpyridine-derivative that forms a six-membered ring (**BPF**: d(N→B) = 1.627(2) Å[17]). Compared to **SiBMes$_2$**, the carbon-boron bond to the vinyl carbon atom (d(B1-C12) = 1.623(3) Å) is substantially longer, while the adjacent C=C-double bond (d(B12-C13) = 1.346(3) Å) appears shortened. These observations are in agreement with transition to a tetracoordinated carbon atom, while the variation of the double-bond-length lies within the typical variation for this type of system.[48]

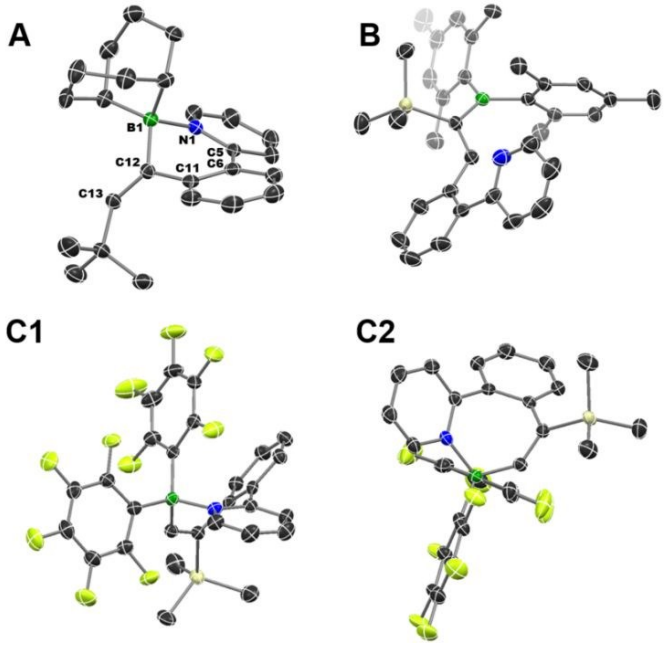

Figure 3. Crystal structures of vinyl-boranes. **A:** ***t*BuBBN**; **B: SiBMes$_2$**; **C1/C2:** side- and top-down view of **SiBPF**. Structures shown at 55% probability level. Hydrogen atoms have been omitted for clarity. Representative labels shown for ***t*BuBBN** in **A**.

Optical and electrochemical properties: The optical absorption properties differ somewhat from those of their styryl-pyridine-derived analogous. **SiBMes$_2$** and **SiBPF** exhibit redshifted λ_{max} values of 356 and 360 nm. However, their absorption falls of sharply, resulting in gaps of 3.44 and 3.48 eV, respectively. These latter values are close to those of the previously reported compounds **BPh$_2$** and **BPF** (**BPh$_2$**: λ_{max} = 306 nm, E_g^{opt} = 3.42 eV; **BPF**: λ_{max} = 310 nm, E_g^{opt} = 3.50 eV). ***t*BuBBN** (λ_{max} = 339 nm (shoulder band), E_g^{opt} = 3.09 eV) exhibits the lowest optical gap in the series. Indeed, the optical gap of ***t*BuBBN** is almost 0.1 eV lower than even that of its derivative **BBN** (**BBN**: λ_{max} = 303 nm, E_g^{opt} = 3.17 eV), owed to a distinct shoulder band centered on 339 nm. **SiBPF** is the only borane in the current and previous surveys that shows fluorescence with an emission maximum at 420 nm. Curiously, **SiBMes$_2$** also turned out to be non-fluorescent, even though structurally related vinyl-boranes are.[48b,37]

The electrochemical properties of the three boranes were also studied, to elucidate the impact of the extension of the

View Article Online
DOI: 10.1039/C9DT01555H

conjugated system, and the changes in molecular architecture. For ***t*BuBBN** reversible electrochemical reduction was observed with a peak potential at -2.50 V vs. FcH/FcH$^+$. **SiBMes$_2$** shows a reversible reduction at -2.37 V vs. FcH/FcH$^+$, followed by a second, irreversible reduction at -2.65 V. **SiBPF** exhibits the highest electron affinity with a peak potential at -2.21 V, but undergoes only quasi-reversible reduction. The reduction potentials of ***t*BuBBN** and **SiBPF** are therefore close to those of their phenylpyridine-derived analogues (**BBN**: E_{red}^{p} = -2.25 V, **BPF**: -2.20 V[17]). The reduction potential of **SiBMes$_2$** lies within the typically range Mes$_2$B-functionalized arenes,[49] and also agrees with the electron affinity of its diphenylboryl-analogue (**BPh$_2$**: E_{red}^{p} = -2.40 V[17]). Overall, these compounds offer comparable electrochemical properties despite their more extended π-systems.

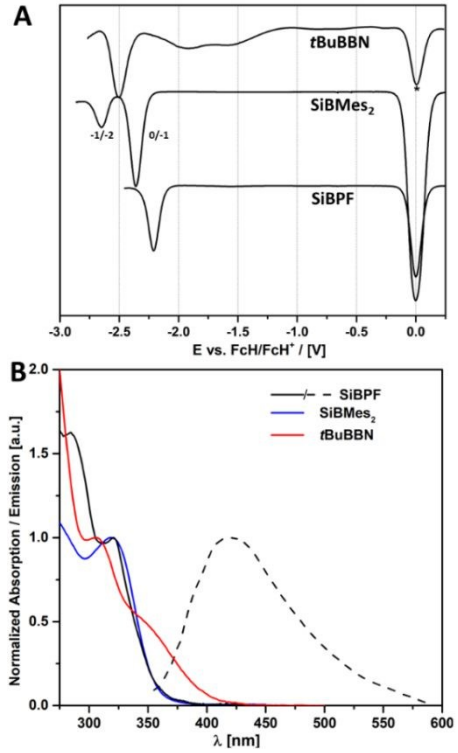

Figure 4. A Square-wave voltammetry scans of vinyl-boranes ***t*BuBBN**, **SiBMes$_2$**, and **SiBPF**. Recorded in THF with 0.1M NBu4PF6 as supporting electrolyte at a scan rate of 200 mV/s. * internal standard Ferrocene. **B** Normalized UV-vis-absorption spectra of ***t*BuBBN**, **SiBMes$_2$**, and **SiBPF** (solid black line), and emission spectrum of **SiBPF** (dashed black line) recorded in THF.

DFT calculations: To elucidate the origin of the optical properties of these compounds, the structures were also simulated by DFT, optical transitions were calculated by TD-DFT, and the resulting UV-vis absorption spectra were simulated (see Figure S5 in the ESI). These calculations showed that the lowered optical gap in ***t*BuBBN** compared to **BBN** could be attributed to a combination of the properties of the BBN-moiety, and the extension of the π-system onto the vinyl group. According to the calculations, the experimentally observed longest wavelength absorption band is composed of two comparatively weakly populated transitions (ES1: E = 3.69 eV / 336 nm, f = 0.052, 92% HOMO-to-LUMO; ES2: E = 4.03 eV / 308 nm, f = 0.038, 10% HOMO-2-to-LUMO + 81% HOMO-1-to-LUMO). The LUMO is a pure π*-type orbital delocalized throughout the phenylpyridine-ring system, with only minor contributions from the vinylic side chain. In contrast, HOMO, HOMO-1 and HOMO-2 show strong σ-type contributions of boron-carbon-bonds in the BBN frame, as well as π-type contributions of the vinylic bond in the side chain, while only weak π-delocalization onto the phenyl-ring is present in the HOMO and the HOMO-1. The σ-character of the occupied orbitals and very limited spatial overlap with the LUMO explain the weak population of the lowest energy transitions. Overall, the extension of the conjugation into the sidechain both raises the HOMO and somewhat lowers the LUMO of ***t*BuBBN** ($HOMO^{DFT}$ = -7.18 eV, $LUMO^{DFT}$ = -1.36 eV) compared to **BBN** ($HOMO^{DFT}$ = -7.26 eV, $LUMO^{DFT}$ = -1.31 eV). Notably, this is another example for a 9BBN-containing ladder borane wherein the σ-type contributions to the HOMO render the lowest energy transition formally forbidden and thus only weakly populated.[17,18,19]

For **SiBMes$_2$** the calculations predict the main absorption band to be composed of two rather strongly populated transitions, that are HOMO-1- and HOMO-to-LUMO in character (ES1: E = 4.02 eV / 308 nm, f = 0.129, 27% HOMO-1-to-LUMO + 39 % HOMO-to-LUMO; ES2: E = 4.20 eV / 296 nm, f = 0.144, 47 % HOMO-1-to-LUMO + 31 % HOMO-to-LUMO). The LUMO in this system is a π*-orbital and shows strong contributions from the empty p_z-orbital on boron, but is also delocalized across the vinyl-group and throughout the phenyl-pyridine π-system. The HOMO and HOMO-1, however are mainly composed of the π-

Table 3. Structural and electronic properties of vinyl-boranes.

Borane	Space Group	N1→B1	N1-C5-C6-C11	C5–C6	C12–B1 CHC-B	CH=CB	λ_{max}	$E_g^{opt[a]}$		$E_p^{red[b]}$	DFT[c] N→B	*open* vs. *closed*[d]	^{11}B NMR[e]
		[Å]	[°]	[Å]	[°]	[Å]	[nm]	[nm]	[eV]	[V]	[Å]	[kJ/mol]	[kJ/mol]
***t*BuBBN**	P121/c1 monoclinic	1.662(4)	25.7(4)	1.469(4)	1.621(4)	1.352(4)	339[f]	401	3.09	-2.50r	1.672	+45	-0.0 -2.7 (THF)
SiBPF	P-1(2) triclinic	1.640(2)	-55.6(3)	1.486(3)	1.623(3)	1.346(3)	321	360	3.44	-2.21qr	1.637	+90	-4.7
SiBMes$_2$	P121/n monoclinic		26.0(2)	1.482(3)	1.563(3)	1.354(2)	318	356	3.48	-2.37r -2.65i	--	--	78.4 (CD_2Cl_2)

[a] Derived from absorption onset of UV-vis spectra in recorded in THF-solution. [b] Peak potentials derived by square wave voltammetry. i/r: (ir)-reversibility as observed by cyclic voltammetry. [c] Optimized by DFT at the M06-2X/6-31G(d,p) level of theory. [d] Destabilization of non-coordinated ***open*** conformer over N→B-ladder conformer. [e] Recorded in C_6D_6, unless stated otherwise. [f] Shoulder band. Maximum derived by deconvolution.

orbitals of the electron rich mesityl-rings, with only partial contributions from the vinyl-group and the phenyl-ring in the HOMO-1.

Lastly, for **SiBPF** the TD-DFT calculations predict a lowest energy transition comparable in energy as those for **$SiBMes_2$**, which is in agreement with the experimental data. The optical absorption is dominated by a single transition that is near exclusively HOMO-to-LUMO in character (ES1: E = 4.12 eV / 301 nm, f = 0.071, 86% HOMO-to-LUMO, 5 % HOMO-to-LUMO+1). Both LUMO and LUMO+1 are π-orbitals delocalized within the phenylpyridine-ring system, but with substantially lower contributions from the phenyl-ring, while the HOMO represents a π-orbital delocalized across the phenyl-ring and the vinylic side chain. Notably, these calculations predict that an ***open*** conformer would exhibit a much more redshifted absorption (ES1: E = 3.35 eV / 370 nm, f = 0.032, 19 % HOMO-1-to-LUMO, 69 % HOMO-to-LUMO).

The above results present a new class of substrates suitable for conversion in N→B-ladder boranes by hydroboration. The isolation and structural characterization of ***t*BuBBN** proves that α-borylation can be sterically enforced, and N→B-ladder formation is still possible. Steric pressure of a TMS-group is evidently insufficient, however due to the dominating β-silicon effect. In future works, the use of bulkier silyl-substituents,[45] and indeed less bulky alkyl-groups,[39,50] may be explored to generate this kind of molecular structure.

Conclusions

In summary, we have prepared a series of new boranes capable of forming N→B-heterocycles through intramolecular coordination. Through systematic variation of the substituents on boron in an established 2-phenylpyridine-derived system we completed the whole series of haloboranes (previously: **BCl_2**,[17] newly reported herein: **BBr_2**, **BF_2**, **BI_2**), and also made a pseudo-halide derivative (**B(CN)(NC)**) available. To the best of our knowledge, very few isocyanoborates have been reported in the literature, while **B(CN)(NC)** is the first example of a neutral isocyano-borane. However, it is not quite certain at this point, whether the **B(CN)(NC)** emergences only in the solid state, or is also present in solution.

We have also introduced 2'-alkynyl-substituted 2-phenyl-pyridines as a new class of substrates. Hydroboration of a *tert*-butyl-terminated alkyne lead to the isolation of a new π-extended ladder borane (***t*BuBBN**), wherein the desired regioselectivity is preserved, while in the hydroboration of trimethylsilyl-terminated substrates, the regioselectivity is reversed. Borylation either lead to the formation of an isomer incapable of ladder formation (**$SiBMes_2$**), or, after a strain reducing 1,2-silyl-shift (**SiBPF**) to formation of an 1,2-azaborepine by intramolecular N→B-coordination.

Analyses of the new boranes by electrochemical methods and UV-vis-spectroscopy were complemented by DFT calculations. We showed that systematic variation of the substituents on boron allows for the incremental variation of the electron affinity of the phenylpyridine-model system over a range of > 0.7 eV between alkylboranes (**BMe_2**, **BBN**) and **B(CN)(NC)**. Indeed, **B(CN)(NC)** shows the strongest N→B-bond (≈ 175 kJ/mol), and highest electron-affinity observed so far, while in the sterically encumbered ***t*BuBBN** N→B-coordination is still predominant even though the N→B-bond is the weakest yet (≈ 45 kJ/mol).

With regard to potential applications of these compounds in organic electronics, we can also state that several of the investigated boranes exhibit sufficient stability to be handled and processed under ambient conditions. The **BF_2**- and **BCl_2** derivatives are bench-stable as solids, and can be handled in solution over short periods of time, while **BBr_2** and **BI_2** are not stable under these conditions. The vinyl-boranes **$SiBMes_2$** and **SiBPF** are insensitive against ambient conditions even in solution.

These results are fully consistent with our previous reports and significantly expand both the scope and the knowledge base for a further exploration of this chemistry.

Experimental Section

Materials and Instrumentation

All reactions and manipulations of sensitive compounds were carried out under an atmosphere of pre-purified argon using either Schlenk techniques or an inert-atmosphere glovebox (MBraun Labmaster). Dichloromethane was purified using a solvent purification system (MBraun; alumina / copper columns). Hexane was dried by distillation from CaH_2 under argon atmosphere prior to use. Other commercially available solvent and reagents (Merck, VWR, Acros, Alfa Aesar) were either used as obtained or purified by standard procedures.[51] ^{1}H-, and ^{13}C-NMR spectra were recorded at 293 K on a Bruker Avance DRX 400 (400 MHz) spectrometer or a Bruker Avance 500 AMX (500 MHz). Solution ^{1}H and ^{13}C NMR spectra were referenced internally to the solvent residual signals.[52] Individual signals are referred to as singlet (s), doublet (d), and multiplet (m). High resolution mass spectrometry measurements were performed on a Bruker SolariX FTMS using MALDI (Matrix Assisted Laser Desorption Ionization) as ionization method with *trans*-2-[3-(4-tert-butylphenyl)-2-methyl-2-propenylidene]malononitrile (DCTB) as matrix. UV-visible absorption spectra and photoluminescence spectra were acquired on a Perkin Elmer Lambda 19 UV-vis/NIR spectrometer and a Perkin Elmer LS 55 fluorescence spectrometer, respectively.

Deconvolution of UV-vis spectra was performed with OriginPro 9.0G. Melting points were measured on a Büchi M 565 melting point apparatus with a heating rate of 1 °C/min. Infrared spectroscopy was performed on a Perkin Elmer Spektrum BX FT-IR System (Software: Spektrum v3.02 Version 3.02.01, Perkin Elmer). Crystallography: X-ray diffraction intensities were collected an Agilent Technologies SuperNova single-crystal X-ray diffractometer at 150 K using Mo-Kα radiation, and the structures were solved using direct methods (SIR92 or Shlexs-2014), completed by subsequent difference Fourier syntheses, and refined by full-matrix least-squares procedures. Semi-empirical absorption corrections from equivalents (Multiscan)

were carried out. CCDC 1899857 through 1899864 contain the supplementary crystallographic data for **BBr_2**, **BF_2**, **BI_2**, **B(CN)(NC)**, ***t*BuBBN**, **$SiBMes_2$**, **SiBPF**, **and 2b*$HBMes_2$**. These data can be obtained free of charge from the Cambridge Crystallographic Data Centre via www.ccdc.cam.ac.uk/data_request/cif, and are also included at the end of this document. Computational Details: Quantum chemical calculations were performed on the bwForCluster JUSTUS at the University of Ulm, using release B.01 of the Gaussian16 program package. Geometry optimizations were performed at the M06-2X/6-31G(d,p)-level. All converged structures were found to be local energetic minima, as established by frequency calculations. Electronic and optical properties were simulated using the M06-2X functional and base set 6-311+G(d,p) in the gas phase Kohn-Sham frontier orbitals were plotted using GaussView 5.0. Absorption spectra were simulated using GaussSum 3.0[53] at a half-width at half height of 0.62 eV (5000 cm^{-1}). The above combination of functionals and base sets was chosen, because M06-2X functional reproduces non-covalent coordinative interactions in organoboranes well. Also, the same level of theory was used in a previous comprehensive publication on the same basic system,[17] and the results can therefore be compared directly.

Synthetic Procedures

Synthesis of (2-*o*-bromophenyl)-1-trimethylsilylacetylene (BrTMS): This compound was synthesized according to modified literature procedure.[54] To a solution of 1-bromo-2-iodobenzene (2.93 g, 10.4 mmol), CuI (60 mg, 0.31 mmol) and $PdCl_2(PPh_3)_2$ (218 mg, 0.31 mmol) in 15.6 mL dry NEt_3 TMS-acetylene (1.22 g, 12.4 mmol) was added and the mixture was stirred at room temperature for 19 h. After removal of the solvent under reduced pressure the residue was dissolved in ethyl acetate and the organic phase was washed with an aqueous $NaHCO_3$ and a NaCl-solution. The organic phase was dried over $MgSO_4$ followed by removal of the solvent under reduced pressure. The residue was purified by silica column chromatography using petroleum spirit as eluent furnishing the product as yellow oil in quantitative yield (2.64 g).

^{1}H NMR (400 MHz, $CDCl_3$): δ = 7.58 – 7.55 (m, 1H, C1-H), 7.49 (ddd, *J* = 7.7, 1.8, 0.4 Hz, 1H, C4-H), 7.26 – 7.22 (m, 1H, C3-H), 7.15 (ddd, *J* = 8.0, 7.5, 1.8 Hz, 1H, C2-H), 0.28 (s, 9H, C5-H) ppm. ^{13}C NMR (101 MHz, $CDCl_3$): δ = 133.74, 132.49, 129.71, 127.03, 125.90, 125.36, 103.15 (C6), 99.77 (C7), -0.01 (C5) ppm.

Synthesis of (1-tert-butyl)-(2-bromophenyl)acetylene (Br*t*Bu): This synthesis followed a modified literature procedure.[55] A 500 mL Schlenk-flask was charged with 1-bromo-2-iodobenzene (19.9 g, 70.3 mmol), and triethylamine (100 mL). The mixture was degassed by bubbling argon inside the solution for 30 min with vigourous stirring, and subsequently a suspension of 1.0 g (1.4 mmol) of $PdCl_2(PPh_3)_2$ and 0.5 g (2.8 mmol) of CuI in a few mililiters of anhydrous THF was added. Cold (-20 °C) 3,3-Dimethylbutyne (7.0 mL, 85.2 mmol) was added last, the reaction vessel was sealed and stirred at ambient temperature for 19 h. Subsequently, the reaction mixture was filtered over Celite, solvent and triethylamine were removed under vacuum and the residue was purified by column chromatography and distillation. **Br*t*Bu** was obtained as pale yellow oil in a yield of 12% (1.9 g, 8.1 mmol).

^{1}H-NMR ($CDCl_3$, 400 MHz): δ = 7.55 (ddd, $^3J_{H,H}$ = 8.0 Hz, $^4J_{H,H}$ = 1.3 Hz, $^5J_{H,H}$ = 0.4 Hz, 1H, C1-H), 7.41 (ddd, $^3J_{H,H}$ = 7.7 Hz, $^4J_{H,H}$ = 1.8 Hz, $^5J_{H,H}$ = 0.4 Hz, 1H, C4-H) 7.23 – 7.17 (m, 1H, C3-H), 7.12 – 7.08 (m, 1H, C2-H), 1.35 (s, 9H, $(CH_3)_3$) ppm. ^{13}C-NMR ($CDCl_3$, 101 MHz) : δ =133.14, 132.36, 128.69, 126.96, 126.12, 125.87, 103.73, 78.10, 30.97 (3C, $(CH_3)_3$), 28.40 ppm. MS (EI, 70 eV): m/z calcd for $C_{12}H_{13}Br$: 236.02 Da; found: 142.10 (100) Da [M -CH_3 - Br]$^+$, 236.05 (17) Da [M]$^+$.

Synthesis of 2-(2-((trimethylsilyl)ethynyl)phenyl)pyridine (2b): BrTMS (1.97 g, 7.8 mmol) was dissolved in 9 mL dry THF and the solution was cooled to -78 °C. A 1.6 M solution of *n*BuLi (4.95 mL, 7.9 mmol) was added dropwise and the solution was stirred at -78 °C for 2 h followed by the addition of $ZnCl_2$ (1.08 g, 7.92 mmol). The mixture was stirred at -78 °C for 45 min, after which the solution was allowed to reach room temperature. After the addition of $PdCl_2(PPh_3)_2$ (218 mg, 0.31 mmol) and 2-bromopyridine (1.53 g, 9.71 mmol) the solution was stirred at room temperature for 12 h. The reaction mixture was adsorbed on silica and purified by flash-gel silica column chromatography using an eluent gradient of petroleum spirit/ethyl acetate 20/1 to 10/1 which furnished the product as yellow oil (1.19 g, 61%).

^{1}H NMR (400 MHz, $CDCl_3$, 25 °C): δ = 8.72 (ddd, *J* = 4.9, 1.7, 1.0 Hz, 1H, C1-H), 7.99 (dt, *J* = 8.0, 1.0 Hz, 1H, C7-H), 7.76 (dd, *J* = 7.8, 1.3 Hz, 1H), 7.72 (td, *J* = 7.7, 1.8 Hz, 1H), 7.59 (dd, *J* = 7.7, 1.4 Hz, 1H), 7.43 (td, *J* = 7.6, 1.4 Hz, 1H), 7.34 (td, *J* = 7.6, 1.4 Hz, 1H), 7.29 – 7.24 (m, 1H), 0.16 (s, 9H, C14-H) ppm. ^{13}C NMR (101 MHz, $CDCl_3$, 25 °C): δ = 157.36 (C5), 149.34 (C1), 142.35, 135.75 (C6), 133.58, 129.73, 129.09, 128.34, 124.82, 122.41, 121.25, 104.54 (C12), 98.24 (C13), -0.17 (C14) ppm. HR-MS (ESI): m/z calcd for $C_{16}H_{18}NSi^+$ [M+H]$^+$: 252.1203 Da; found: 252.1203 Da.

Synthesis of 2-(2-((*tert*-butyl)ethynyl)phenyl)pyridine (2a): A Schlenk tube was charged with a solution of 1.3 g (5.5 mmol) of 1-bromo-2-(3,3-dimethylbut-1-in-1-yl)benzene (**Br*t*Bu**) in dry benzene and 3.5 g (0.3 mmol) of $Pd(PPh_3)_4$ and 2.8 g of (7.6 mmol) 2-(tri-*n*-butylstannyl)pyridine were added. The tube was sealed, and the reaction mixture was stirred for 3 days at 110 °C. Subsequently, the solvent was removed under vacuum, and the crude product was purified by column chromatography (SiO_2, hexanes/ethyl acetate 1:1, v/v), followed by distillation. **2a** was obtained in 11% yield (142 mg, 0.6 mmol) as a pale brown oil.

b.p. = 45 °C at 3×10^{-3} mbar. ^{1}H-NMR ($CDCl_3$, 400 MHz): δ = 8.70 (ddd, $^3J_{H,H}$ = 4.8 Hz, $^4J_{H,H}$ = 1.9 Hz, $^5J_{H,H}$ = 1.0 Hz, 1H, C1-H), 7.97 – 7.95 (m, 1H, C4-H), 7.73 – 7.67 (m, 2H, C7-H, C3-H), 7.49 (ddd, $^3J_{H,H}$ = 7.5 Hz, $^4J_{H,H}$ = 1.5 Hz, $^5J_{H,H}$ = 0.6 Hz, C10-H), 7.38 – 7.34 (m, 1H, C8-H), 7.32 – 7.27 (m, 1H, C9-H), 7.24 – 7.21 (m, 1H, C2-H), 1.20 (s, 9H, $(CH_3)_3$) ppm. ^{1}H-NMR (THF, 400 MHz): δ = 8.64 (ddd, $^3J_{H,H}$ = 4.8 Hz, $^4J_{H,H}$ = 1.9 Hz, $^5J_{H,H}$ = 1.0 Hz, 1H, C1-H), 8.10 – 8.07 (m, 1H, C4-H), 7.83 (ddd, $^3J_{H,H}$ = 7.8 Hz, $^4J_{H,H}$ = 1.5 Hz, $^5J_{H,H}$ = 0.5 Hz, 1H, C7-H), 7.75 – 7.70 (m, 1H, C3-H), 7.44 (ddd, $^3J_{H,H}$ = 7.5 Hz, $^4J_{H,H}$ = 1.5 Hz, $^5J_{H,H}$ = 0.6 Hz, C10-H), 7.37 – 7.33 (m, 1H, C8-H), 7.30 – 7.26 (m, 1H, C9-H), 7.23 (ddd, $^3J_{H,H}$ = 7.5 Hz, $^4J_{H,H}$ = 4.8 Hz, $^5J_{H,H}$ = 1.1 Hz, 1H, C2-H), 1.24 (s, 9H, $(CH_3)_3$) ppm. ^{13}C-NMR ($CDCl_3$, 101 MHz): δ = 157.94, 149.37, 142.01, 135.30, 132.99,

129.51, 128.12, 127.93, 124.63, 122.07, 101.76, 78.65, 30.71 (CH_3), 28.14 ppm. ^{13}C-NMR (THF, 101 MHz): δ = 157.36, 149.26, 141.96, 134.75, 132.71, 129.67, 127.61, 127.46, 124.02, 121.78, 121.65, 101.00, 79.01, 30.00 (CH_3), 27.89 ppm. MS (EI, 70 eV): m/z calcd for $C_{17}H_{17}N$: 235.14 Da; found: m/z (%) = 220.10 (100) Da [M -CH_3]$^+$, 235.05 (7) Da [M]$^+$.

Synthesis of (*Z*)-2-(2-(1-(9-borabicyclo[3.3.1]nonan-9-yl)-3,3-dimethylbut-1-en-1-yl)phenyl)pyridine (*t*BuBBN): Inside an inert gas glovebox a NMR tube equipped with a Young valve was charged with a solution of 36.1 mg (153 µmol) of **2a** and 244 mg (97.5 µmol) of 9*H*-BBN in 0.5 mL of anhydrous THF-d_8. The tube was sealed and heated for 3 days at 60 °C, when control via NMR indicated full conversion of the starting material. Subsequently, the solvent was removed and the residue was extracted with dry *n*-hexane. The extract was evaporated to dryness, and the resulting crude product was washed through a short column of alumina with toluene under inert conditions. Evaporation of the solvent gave 26.8 mg (75.0 µmol, 49%) of ***t*BuBBN** as a pale yellow solid.

^{1}H-NMR (C_6D_6, 400 MHz): δ = 8.48 (ddd, $^3J_{H,H}$ = 6.0 Hz, $^4J_{H,H}$ = 1.7 Hz, $^5J_{H,H}$ = 0.7 Hz, 1H, C1-H), 7.47 – 7.45 (m, 1H), 7.16 – 7.12 (m, 2H), 7.01 – 6.96 (m, 1H), 6.94 – 6.92 (m, 1H), 6.73 – 6.69 (m, 1H), 6.20 – 6.17 (m, 1H), 6.11 (s, 1H, C13-H), 3.05 – 2.96 (m, 1H, BBN-H), 2.46 – 2.36 (m, 1H, BBN-H), 2.27 – 2.16 (m, 3H, BBN-H), 2.05 – 1.92 (m, 3H, BBN-H), 1.78 – 1.73 (m, 3H, BBN-H), 1.72 – 1.68 (m, 1H, BBN-Bridgehead), 1.32 – 1.29 (m, 1H, BBN-H), 1.12 (s, 9H, $(CH_3)_3$), 0.79 – 0.74 (m, 1H, BBN-Bridgehead) ppm. ^{1}H-NMR (THF, 400 MHz): δ = 8.82 (ddd, $^3J_{H,H}$ = 6.0 Hz, $^4J_{H,H}$ = 1.8 Hz, $^5J_{H,H}$ = 0.7 Hz, 1H, C1-H), 8.07 – 8.03 (m, 1H, C3-H), 7.98 – 7.95 (m, 1H, C4-H), 7.70 – 7.68 (m, 1H, C7-H), 7.47 (ddd, $^3J_{H,H}$ = 7.4 Hz, $^4J_{H,H}$ = 5.9 Hz, $^5J_{H,H}$ = 1.0 Hz, 1H, C2-H), 7.35 – 7.30 (m, 2H, C9-H, C10-H), 7.24 – 7.18 (m, 1H, C8-H), 5.74 (s, 1H, BC-C-H), 2.55 – 2.46 (m, 1H, BBN-H), 2.38 – 2.29 (m, 1H, BBN-H), 2.08 – 1.95 (m, 1H, BBN-H), 1.91 – 1.61 (m, 3H, BBN-H), 1.50 – 1.42 (m, 3H, BBN-H), 1.36 – 1.30 (m, 3H, BBN-H), 1.27 – 1.22 (m, 1H, BBN-Bridgehead H), 0.94 (s, 9H, $(CH_3)_3$), 0.36 – 0.32 (m, 1H, BBN-Bridgehead H) ppm. ^{13}C-NMR (C_6D_6, 101 MHz): δ = 154.61, 146.39, 144.73, 139.98, 138.32, 130.88, 129.95, 128.86, 125.15, 123.05, 121.52 (2C), 42.05 (br C-B), 35.90 (BBN), 34.88, 32.49 (BBN), 32.43 (3C, $(CH_3)_3$), 32.17 (BBN), 30.78 (BBN), 24.94 (BBN), 24.68 (BBN), 23.90 (br, BBN-Bridgehead C), 22.03 (br s, BBN-Bridgehead C) ppm. ^{13}C-NMR (THF, 101 MHz): δ = 155.11, 146.52, 145.55 (C1), 140.16 (C3), 139.54 (C^3-H) , 131.57, 129.92 (C9), 128.83 (C10), 125.70 (C7), 125.57 (C8), 124.25 (C4), 123.02 (C2), 40.94 (br s, C-B), 35.77 (BBN), 34.93, 33.82 (BBN), 32.34 (3C, $(CH_3)_3$), 32.08 (BBN), 30.84 (BBN), 24.76 (BBN), 24.51 (BBN), 22.21 (br s, BBN-Bridgehead C), 20.43 (br s, BBN-Bridgehead C) ppm. ^{11}B-NMR (C_6D_6, 128 MHz): δ = -0.04 (br s) ppm. ^{11}B-NMR (THF, 128 MHz): δ = -2.68 (br s) ppm. MS (EI, 70 eV): m/z calcd for $C_{25}H_{32}BN$: 357.26 Da; found: m/z (%) = 357.20 (22) [M]$^+$.

Synthesis of (Z)-2-(2-(2-(dimesitylboraneyl)-2-(trimethylsilyl)-vinyl)phenyl)pyridine (SiBMes$_2$): Inside the glovebox compound **2b** (31 mg, 0.12 mmol) and $HBMes_2$ (31 mg, 0.12 mmol) were dissolved in 1 mL anhydrous benzene and the solution was heated to 85 °C for 48 h. After removal of the solvent under reduced pressure, the residue was suspended in hexane and the resulting precipitate was removed. The hexane solution was concentrated and the product was crystallized at -30 °C yielding the product as colorless crystals (20 mg, 32%).

^{1}H NMR (400 MHz, CD_2Cl_2): δ = 8.46 (ddd, *J* = 4.8, 1.7, 0.9 Hz, 1H, C1-H), 7.65 (br s, 1H, C12-H), 7.62 (td, *J* = 7.7, 1.9 Hz, 1H), 7.57 – 7.53 (m, 1H), 7.47 – 7.39 (m, 3H), 7.29 (dt, *J* = 7.9, 0.9 Hz, 1H), 7.18 (ddd, *J* = 7.6, 4.9, 1.1 Hz, 1H), 6.74 (s, 4H, C17-H), 2.26 (s, 6H, C20-H), 2.11 (s, 12H, C19-H), -0.18 (s, 9H, C14-H) ppm. ^{1}H NMR (400 MHz, C_6D_6): δ = 8.47 (ddd, *J* = 4.8, 1.6, 1.2 Hz, 1H, C1-H), 8.06 (s, 1H, C7-H), 7.63 – 7.57 (m, 2H), 7.16 (m, *J* = 4.5 Hz, 2H), 7.13 – 7.07 (m, 2H), 6.72 (s, 4H, C17-H), 6.67 (m, 1H), 2.29 (s, 12H, C19-H), 2.16 (s, 6H, C20-H), 0.09 (s, 9H, C14-H) ppm. ^{13}C NMR (126 MHz, CD_2Cl_2): δ = 156.50, 149.65, 140.96, 140.42, 138.66, 136.30, 129.84, 129.38, 128.57, 128.52, 128.13, 124.32, 121.93, 23.52 (*o*-CH_3), 21.29 (*p*-CH_3), 1.54 (Si(CH_3)$_3$)ppm.
(C19), 21.45 (C20), 1.70 (C14) ppm. ^{11}B NMR (128 MHz, CD_2Cl_2): δ = 78.39 (br s) ppm.

NMR data for adduct 2b*HBMes$_2$ ^{1}H NMR (400 MHz, C_6D_6): δ = 8.62 – 8.54 (m, 1H), 7.46 (dd, *J* = 6.7, 2.3 Hz, 1H), 7.28 (m, 2H), 6.95 (t, *J* = 7.6 Hz, 1H), 6.89 (br s, 4H, Mes), 6.85 – 6.77 (m, 2H), 6.76 – 6.54 (m, 1H, HB-), 6.37 (t, *J* = 6.4 Hz, 1H), 2.30 (br s, 6H, Mes-CH_3), 2.15 (br s, 12H, Mes-CH_3), 0.09 (s, 9H, Si-CH_3) ppm. ^{11}B NMR (128 MHz, C_6D_6): δ = 3.85 (br s) ppm.

Synthesis of (E)-2-(2-(2-(bis(perfluorophenyl)boraneyl)-1-(trimethylsilyl)vinyl)phenyl)pyridine (SiBPF): Inside the glovebox **2b** (87 mg, 0.3 mmol) and Pier's Borane (109 mg, 0.3 mmol) were dissolved in 1.6 mL dry benzene and the solution was stirred at 85 °C for 27 h. The solvent was removed under reduced pressure and the residue was purified by silica column chromatography using petroleum spirit/ethyl acetate 5/1 as eluent furnishing the product as colorless solid (83 mg, 40%). Crystals suitable for XRD-analysis were obtained by crystallization from a hexane solution at -30 °C.

^{1}H NMR (400 MHz, C_6D_6) δ 7.91 – 7.85 (m, 1H, C1-H), 7.69 (dd, *J* = 5.0, 2.8 Hz, 1H, C7-H), 7.23 (dd, *J* = 7.8, 1.0 Hz, 1H), 6.88 – 6.82 (m, 1H), 6.82 – 6.76 (m, 2H), 6.74 – 6.65 (m, 2H), 6.27 (ddd, *J* = 7.6, 6.2, 1.5 Hz, 1H), 0.22 (s, 9H, C14-H) ppm. ^{13}C NMR (101 MHz, CD_2Cl_2): δ = 163.74, 158.22, 146.63, 146.60, 144.73, 144.11, 141.39, 134.37, 131.91, 131.88, 130.24, 129.77, 127.68, 125.54, 123.91, 0.07 (C14) ppm. ^{11}B NMR (128 MHz, C_6D_6): δ = -4.67 (br s) ppm. ^{19}F NMR (376 MHz, C_6D_6): δ = -129.79 (br s, 1F), -130.08 (dd, *J* = 23.9, 8.6 Hz, 1F), -132.58 (br s, 1F), -137.73 – -137.96 (m, 1F), -157.28 (t, *J* = 21.1 Hz, 1F), -162.00 (t, *J* = 20.6 Hz, 1F), -163.88 (br s, 1F), -164.64 (br s, 1F), -166.75 (dddd, *J* = 23.6, 20.8, 8.7, 2.5 Hz, 1F), -169.05 – -169.26 (m, 1F) ppm.

Synthesis of 2-(2-(1-(dibromoboryl)-2-methylpropyl)phenyl)-pyridine (BBr$_2$): Inside an inert gas glovebox a Schlenk tube was charged with a solution of 1.0 g (4.8 mmol) 2-(*ortho*-styryl)pyridine in 50 mL of dry toluene. The Schlenk tube was taken out of the glove box, and 2.0 mL (18.2 mmol) $HBBr_2$•SMe_2 were slowly added, and the reaction mixture was stirred at ambient temperature overnight. The resulting orange solution was evaporated to dryness, the residue was dried at 120 °C under oil pump vacuum for 3 h. Subsequently, the residue was extracted with hot toluene, and the combined extracts were concentrated until crystallization of the product set in. Harvesting of the crystals yielded 1.0 g (24.0 mmol, 56%) of **BBr$_2$** as a colorless solid.

View Article Online DOI: 10.1039/C9DT01555H

^{1}H-NMR (C_6D_6, 400 MHz): δ = 9.50 (psd, $^3J_{H,H}$ = 6.2, 1H, C1-H), 7.23 – 7.17 (m, 2H, C7-H, C10-H), 7.16 – 7.10 (m, 1H, C9-H), 7.05 – 7.01 (m, 1H, C8-H), 6.95 (psd, $^3J_{H,H}$ = 8.2, 1H, C4-H), 6.77 – 6.73 (m, 1H, C3-H), 6.29 – 6.26 (m, 1H, C2-H), 3.03 – 2.94 (m, 1H, $CH(CH_3)_2$), 2.94 – 2.93 (br m, 1H, B-CH), 0.92 (d, $^3J_{H,H}$ = 6.9 Hz, 3H, CH_3), 0.14 (d, $^3J_{H,H}$ = 6.8 Hz , 3H, CH_3) ppm. ^{13}C-NMR (C_6D_6, 101 MHz): δ = 152.90 (C5), 145.68 (C1), 142.68 (C11), 142.30 (C3), 133.85 (C10), 131.59 (C9), 130.33 (C6), 127.24 (C7), 126.50 (C8), 123.23 (C2), 122.40 (C4), 43.97 (br, C-B), 32.17 ($CH(CH_3)_2$), 23.69 (CH_3), 17.28 (CH_3) ppm. ^{11}B-NMR (C_6D_6, 128 MHz): δ = 4.89 (br s) ppm. MS (EI, 70 eV): m/z calcd for $C_{15}H_{16}BBr_2N$: 378.97Da; found: m/z (%) = 377.30 (1) $[M]^+$.

Synthesis of 2-(2-(1-(difluoroboryl)-2-methylpropyl)phenyl)-pyridine (BF_2): In an inert gas glove box 25.3 mg (0.1 mmol) silver hexafluorophosphate and 30.0 mg (0.1 mmol) **BCl_2** were each dissolved in ca. 1 mL of dry dichloromethane. The solutions were added together, and the resulting suspension was stirred at ambient temperature for 17h. Subsequently, the solvent was removed, the residue was washed with dry hexane, and extracted with dry toluene. Removal of the solvent yielded 23.9 mg (0.1 mmol, 92%) BF_2 as colorless solid.

When the procedure was performed analogously using 4.5 equivalents of silver(I) fluoride (AgF) and stirring for 50h, **BF_2** was obtained in 67% yield.

^{1}H-NMR (C_6D_6, 400 MHz): δ = 9.48 (psd, $^3J_{H,H}$ = 6.3, 1H, C1-H), 7.21 – 7.07 (m, 3H, C7-H, C10-H, C9-H) 7.02 – 6.98 (m, 1H, C8-H), 6.90 (psd, $^3J_{H,H}$ = 8.2, 1H, C4-H), 6.68 – 6.64 (m, 1H, C3-H), 6.22 – 6.18 (m, 1H, C2-H), 3.03 – 2.94 (m, 1H, $CH(CH_3)_2$), 2.93 – 2.90 (br m, 1H, B-CH), 0.90 (d, $^3J_{H,H}$ = 6.9 Hz, 3H, CH_3), 0.13 (d, $^3J_{H,H}$ = 6.8 Hz , 3H, CH_3) ppm. ^{1}H-NMR (CD_2Cl_2, 400 MHz): δ = 8.79 (psd, $^3J_{H,H}$ = 5.9 Hz, 1H, C1-H), 8.20 – 8.16 (m, 1H, C3-H) 8.07 (psd, $^3J_{H,H}$ = 8.5 Hz, 1H, C4-H), 7.80 (psd, $^3J_{H,H}$ = 5.9 Hz, 1H, C7-H), 7.62 – 7.58 (m, 1H, C2-H), 7.45 – 7.41 (m, 1H, C9-H), 7.36 – 7.32 (m, 2H, C8-H, C10-H), 1.88 (br m, 1H, $CH(CH_3)_2$), 1.71 – 1.62 (m, 1H, B-CH), 0.83 (d, $^3J_{H,H}$ = 6.7 Hz, 3H, CH_3), 0.52 (d, $^3J_{H,H}$ = 6.7 Hz , 3H, CH_3) ppm. ^{13}C-NMR (C_6D_6, 101 MHz): δ = 152.90 (C5), 145.68 (C1), 142.65 (C11), 142.30 (C3), 133.85 (C10), 131.59 (C9), 130.33 (C6), 127.24 (C7), 126.50 (C8), 123.23 (C2), 122.40 (C4), 43.97 (br, C-B), 32.17 ($CH(CH_3)_2$), 23.69 (CH_3), 17.28 (CH_3) ppm. ^{13}C-NMR (CD_2Cl_2, 101 MHz): δ = 154.11 (d, $^3J_{C,F}$ = 2.5 Hz, C5), 145.76 (d, $^3J_{C,F}$ = 7.2 Hz, C11), 143.05 (C3), 141.59 (d, $^3J_{C,F}$ = 12.5 Hz, C1), 133.95 (d, $^4J_{H,H}$ = 2.2 Hz, C10), 131.53 (C9), 129.79 (C6), 127.28 (C8), 126.51 (C7), 124.12 (C2), 123.20 (d, $^4J_{C,F}$ = 2.5 Hz, C4), 39.15 (br s, C-B), 30.92 (d, $^2J_{C,F}$ = 6.8 Hz, $CH(CH_3)_2$), 22.40 (d, $^4J_{H,H}$ = 2.7 Hz, CH_3), 21.58 (CH_3) ppm. ^{11}B-NMR (C_6D_6, 128 MHz): δ = 6.66 (br s) ppm. ^{11}B-NMR (CD_2Cl_2, 128 MHz): δ = 6.08 (br s) ppm. ^{19}F-NMR (C_6D_6, 376 MHz): δ = -148.03 (br s, 1F), -162.06 (br s, 1F) ppm. ^{19}F-NMR (CD_2Cl_2, 376 MHz): δ = -147.41 (br s, 1F), -162.04 (br s, 1F) ppm.

Synthesis of 2-(2-(1-(diiodoboryl)-2-methylpropyl)phenyl)-pyridine (BI_2): Inside the glovebox **BCl_2** (80 mg, 0.3 mmol) and BI_3 (206 mg, 0.5 mmol) were dissolved in 1 mL dry benzene and the solution was stirred at room temperature for 48 h. The suspension was concentrated under reduced pressure before hexane was added. After removal of the supernatant and washing of the precipitate for four times the pale-yellow solid was dissolved in DCM and precipitated once again in hexane. After removal of the supernatant and drying under reduced pressure the product was obtained as pale yellow solid (105 mg, 81%).

^{1}H NMR (400 MHz, C_6D_6): δ = 9.70 (dd, *J* = 6.2, 1.0 Hz, 1H), 7.11 (td, *J* = 6.8, 2.5 Hz, 3H), 7.02 – 6.96 (m, 1H), 6.78 (d, *J* = 8.1 Hz, 1H), 6.57 (ddd, *J* = 9.2, 7.9, 1.6 Hz, 1H), 6.06 (ddd, *J* = 7.5, 6.4, 1.4 Hz, 1H), 3.10 – 2.99 (m, 1H, $CH(CH_3)_2$), 2.91 (d, *J* = 2.3 Hz, 1H, B-CH), 0.85 (d, *J* = 6.9 Hz, 3H; CH_3), 0.08 (d, *J* = 6.9 Hz, 3H, CH_3) ppm. ^{11}B NMR (128 MHz, C_6D_6): δ = -12.71 (br s) ppm. ^{13}C NMR (101 MHz, C_6D_6): δ = 152.26, 149.03, 142.59, 142.24, 133.50, 131.72, 130.39, 127.31, 126.60, 123.35, 122.40, 34.45 ($CH(CH_3)_2$), 23.74 (CH_3), 17.05 (CH_3).

Synthesis of 2-(2-(1-(dimethylboryl)-2-methylpropyl)phenyl)-pyridine (BMe_2): Under inert gas conditions, 60.0 mg (0.2 mmol) of **BCl_2** were dissolved in 10 mL of dry THF, and cooled to -78°C. A solution of Methylmagnesiumchloride (3M in THF, 0.2 mL, 0.5 mmol) was slowly added to give a yellow solution. The mixture was stirred for 2 h at -78 °C, and was then warmed ambient temperature, and quenched by addition of iso-propanol. The solvent was removed, and the residue was taken up in toluene and the extract was washed through a short column of alumina. Removal of the solvent yielded 47.6 mg (0.2 mmol, 95%) of **BMe_2** as colorless solid.

^{1}H-NMR (C_6D_6, 400 MHz): δ = 8.25 (dd, $^3J_{H,H}$ = 5.9, $^4J_{H,H}$ = 1.7, 1H, C1-H), 7.31 (dd, $^3J_{H,H}$ = 7.5, $^4J_{H,H}$ = 1.4, 1H, C10-H), 7.27 (psd, $^3J_{H,H}$ = 7.8, 1H, C7-H), 7.23 – 7.19 (m, 1H, C9-H), 7.08 – 7.04 (m, 2H, C4-H , C8-H), 6.80 – 6.75 (m, 1H, C3-H), 6.33 – 6.29 (m, 1H, C2-H), 2.36 (heptd, $^3J_{H,H}$ = 6.9, $^3J_{H,H}$ = 3.6, 1H, $CH(CH_3)_2$), 1.98 (d, $^3J_{H,H}$ = 3.6, 1H, B-CH), 1.08 (d, $^3J_{H,H}$ = 6.9 Hz, 3H, CH-CH_3), 0.61 (s, 3H, B-CH_3), 0.30 (d, $^3J_{H,H}$ = 6.9 Hz , 3H, CH-CH_3), 0.15 (s, 3H, B-CH_3) ppm. ^{13}C-NMR (C_6D_6, 101 MHz): δ = 154.43, 147.17, 143.63, 138.86, 134.35, 131.95, 130.56, 126.74, 125.33, 122.71, 121.94, 43.72 (br, C-B), 30.90 (*CH*(CH_3)$_2$), 24.68 (CH_3), 18.96 (CH_3), 13.10 (br, B-CH_3), 9.49 (br s, B-CH_3) ppm. ^{11}B-NMR (C_6D_6, 128 MHz): δ = -2.40 (br s) ppm.

Synthesis of 2-(2-(1-(dicyanoboryl)-2-methylpropyl)phenyl)-pyridine (B(CN)(NC)): Inside the glovebox compound **BCl_2** (22 mg, 0.08 mmol) and TMS-CN (17 mg, 0.17 mmol) were dissolved in 1 mL anhydrous benzene and the solution was heated to 105 °C for 24 h. After removal of the solvent under reduced pressure, the residue was dissolved in DCM and precipitated in hexane twice. After removal of the remaining solvent the product was obtained as brown solid (14 mg, 68%). Single crystals suitable for X-Ray diffraction were obtained by layering a solution of **B(CN)(NC)** in benzene with hexane.

^{1}H NMR (400 MHz, CD_2Cl_2): δ = 9.02 (ddd, *J* = 6.0, 1.5, 0.6 Hz, 1H, C1-H), 8.31 – 8.26 (m, 1H), 8.18 – 8.15 (m, 1H), 7.84 (ddd, *J* = 7.9, 1.4, 0.5 Hz, 1H), 7.71 (ddd, *J* = 7.5, 6.0, 1.4 Hz, 1H), 7.56 (td, *J* = 7.5, 1.4 Hz, 1H), 7.48 – 7.44 (m, 1H), 7.40 (ddt, *J* = 7.5, 1.3, 0.5 Hz, 1H), 2.19 (d, *J* = 4.5 Hz, 1H, B-CH), 2.16 – 2.07 (m, 1H, $CH(CH_3)_2$), 0.95 (d, *J* = 6.8 Hz, 3H, CH_3), 0.27 (d, *J* = 6.8 Hz, 3H, CH_3) ppm.

^{1}H NMR (400 MHz, C_6D_6): δ = 8.46 (dd, *J* = 6.0, 0.7 Hz, 1H, C1-H), 7.09 – 7.03 (m, 1H), 7.00 – 6.92 (m, 3H), 6.69 (d, *J* = 8.1 Hz, 1H), 6.57 – 6.47 (m, 1H), 6.01 (ddd, *J* = 7.4, 6.1, 1.3 Hz, 1H), 2.31 – 2.21 (m, 1H, $CH(CH_3)_2$), 2.14 (d, *J* = 4.1 Hz, 1H, B-CH), 0.81 (d, *J* = 6.8 Hz, 3H, CH_3), 0.15 (d, *J* = 6.9 Hz, 3H, CH_3) ppm. ^{11}B NMR (128

MHz, C_6D_6): δ = -13.02 (br s) ppm. ^{13}C NMR (101 MHz, CD_2Cl_2): δ = = 154.13, 145.91, 144.64, 141.47, 133.41, 132.67, 129.93, 127.92, 127.80, 125.23, 124.54, 38.17 (br, B-CH), 31.74 ($CH(CH_3)_2$), 23.27 (CH_3), 19.35 (CH_3) ppm. IR (KBr): $\tilde{\nu}$ = 2124 cm^{-1} (B-NC), 2211 cm^{-1} (B-CN).

Acknowledgements

The authors thank the German Chemical Industry Fund (FCI) (Liebig scholarship for F. P.) for financial support. We thank Bernhard Mueller for support with X-ray data collection.

Notes and references

1 J. Wang, B. Jin, N. Wang, T. Peng, X. Li, Y. Luo and S. Wang, *Macromolecules*, 2017, **50**, 4629–4638.

2 Reviews: (a) Y. Ren and F. Jäkle, *Dalton Trans.*, 2016, **45**, 13996-14007; (b) F. Jäkle, *Top. Organomet. Chem.*, 2015, **49**, 297-325; (c) A. Doshi and F. Jäkle, *Boron-Containing Polymers - Comprehensive Inorganic Chemistry*, Elsevier Ltd., 2013; (d) F. Jäkle *Chem. Rev.*, 2010, **110**, 3985-4022; (e) F. Jäkle*, Coord.* Chem. *Rev.*, 2006, **250**, 1107-1121; (f) F. Jäkle, in *Encyclopedia of Inorganic Chemistry*, Edt. B. King, Wiley-VCH, New York, 2005, 560-598; (g) C. D. Entwistle and T. B. Marder, *Angew. Chem.*, 2002, **114**, 3051-3056; *Angew. Chem. Int. Ed.*, 2002, **41**, 2927-2931.

3 (a) X. Yin, K. Liu, R. A. Lalancette, Y.-L. Loo and F. Jäkle, *Chem. Sci.,* 2017, **8**, 5497-5505; (b) Y. Zheng, J. Xiong, Y. Sun, X. Pan and J. Wu, *Angew. Chem. Int. Ed.*, 2015, **54**, 12933-12936. *Angew. Chem.*, 2015, **127**, 13125-13128; (c) A. Hübner, T. Kaese, M. Diefenbach, B. Endeward, M. Bolte, H.-W. Lerner, M. C. Holthausen and M. Wagner, *J. Am. Chem. Soc.*, 2015, **137**, 3705-3714; (d) L. Ji, R. M. Edkins, A. Lorbach, I. Krummenacher, C. Brückner, A. Eichhorn, H. Braunschweig, B. Engels, P. J. Low and T. B. Marder, *J. Am. Chem. Soc.*, 2015, **137**, 6750-6753; (e) A. Hübner, A. M. Diehl, M. Diefenbach, B. Endeward, M. Bolte, H.-W. Lerner, M. C. Holthausen and M. Wagner, *Angew. Chem. Int. Ed.*, 2014, **53**, 4832-4835; *Angew. Chem.*, 2014, **126**, 4932-4935; (f) T. Kushida and S. Yamaguchi, *Organometallics*, 2013, **32**, 6654-6657; (g) H. Braunschweig, V. Dyakonov, J. O. C. Jimenez-halla, K. Kraft, I. Krummenacher, K. Radacki, A. Sperlich and J. Wahler, *Angew. Chem. Int. Ed.*, 2012, ***56***, 2977-2980; (h) D. J. H. Emslie, W. E. Piers and M. Parvez, *Angew. Chem. Int. Ed.*, 2003, **42**, 1252−1255; (h) W. J. Grigsby and P. P. Power, *Chem. Eur. J.*, 1997, **3**, 368-375; (j) M. M. Olmstead and P. P. Power, *J. Am. Chem. Soc.*, 1986, **108**, 4235-4236.

4 (a) D. Li, H. Zhang, Y. Wang, *Chem. Soc. Rev.* **2013**, *42*, 8416–8433. *N,O*[2]: (b) Q. Wu, M. Esteghamatian, N. X. Hu, Z. Popovic, G. Enright, Y. Tao, M. D'Iorio and S. Wang, *Chem. Mater.*, 2000, **12**, 79–83; (c) Y. Cui, Q. De Liu, D. R. Bai, W. L. Jia, Y. Tao and S. Wang, *Inorg. Chem.*, 2005, **44**, 601-609. *N,N*[2]: (d) D. Frath, J. Massue, G. Ulrich and R. Ziessel, *Angew. Chem.*, 2014, **126**, 2322–2342; (e) A. Loudet and K. Burgess, *Chem. Rev.*, 2007, **107**, 4891-4932; (f) G. Ulrich, R. Ziessel and A. Harriman, *Angew. Chem.*, 2008, **120**, 1202–1219; *Angew. Chem. Int. Ed.*, 2008, **47**, 1184–1201; (g) R. Ziessel, G. Ulrich and A. Harriman, *New J. Chem.* 2007, **31**, 496–501.

5 S. Wang, D.-T. Yang, J. Lu, H. Shimogawa, S. Gong, X. Wang, S. K. Mellerup, A. Wakamiya, Y.-L. Chang, C. Yang and Z.-H. Lu, *Angew. Chem.*, 2015, **127**, 15289-15293; *Angew. Chem. Int. Ed.*, 2015, **54**, 15074-15078;

6 (a) X. Long, J. Yao, F. Cheng, C. Dou and Y. Xia, *Mater. Org. Chem. Front.*, 2019, **3**, 70-77. (b) Long, Z. Ding, C. Dou and L. Wang, *Mater. Chem. Front.*, 2017, **1**, 852-858. (c) R. Zhao, C. Dou, Z. Xie, J. Liu and L. Wang, *Angew. Chem. Int. Ed.*, 2016, **55**, 5313-5317. (d) X. Long, Y. Gao, H. Tian, C. Dou, D. Yan, Y. Geng, J. Liu and L. Wang, *Chem. Commun.*, 2017, **53**, 1649-1652. (e) X. Long, Z. Ding, C. Dou, J. Zhang, J. Liu and L. Wang, *Adv. Mater.*, 2016, **28**, 6504-6508. (f) Dou, J. Liu and L. Wang, *Sci. China Chem.*, 2017, **60**, 450-459.

7 (a) A. Wakamiya, T. Taniguchi and S. Yamaguchi, *Angew. Chem.*, 2006, **118**, 3242-3245; *Angew. Chem. Int. Ed.*, 2006, **45**, 3170-3173. (b) S. Yamaguchi and A. Wakamiya, *Pure Appl. Chem.*, 2006, **78**, 1413-1424; (c) A. Job, A. Wakamiya, G. Kehr, G. Erker and S. Yamaguchi, *Org. Lett.*, 2010, **12**, 5470-5473; (d) Y.-L. Rao, H. Amarne, L. D. Chen, M. L. Brown, N. J. Mosey and S. Wang, *J. Am. Chem. Soc.* 2013, **135**, 3407-3410; (e) X. Y. Wang, F. D. Zhuang, R. B. Wang, X. C. Wang, X. Y. Cao, J. Y. Wang and J. Pei, *J. Am. Chem. Soc.*, 2014, **136**, 3764-3767. (f) H. Shimogawa, M. Endo, T. Taniguchi, Y. Nakaike, M. Kawaraya, H. Segawa, Y. Murata and A. Wakamiya, *Bull. Chem. Soc. Jpn.*, 2017, **90**, 441-450.

8 R. Hecht, J. Kade, D. Schmidt and A. Nowak-Król, *Chem. Eur. J.*, 2017, **23**, 11620-11628.

9 (a) C. Dou, Z. Ding, Z. Zhang, Z. Xie, J. Liu and L. Wang, *Angew. Chem. Int. Ed.*, 2015, **54**, 3648; (b) Z. Zhang, Z. Ding, C. Dou, J. Liu and L. Wang, *Polym. Chem.*, 2015, **6**, 8029-8035.

10 (a) D. L. Crossley, I. Vitorica-Yrezabal, M. J. Humphries, M. L. Turner, and M. J. Ingleson, *Chem. Eur. J.*, 2016, **22**, 12439-12448; (b) C. Zhu, Z.-H. Guo, A. U. Mu,; Y. Liu, S. E. Wheeler and L. Fang, *J. Org. Chem.*, 2016, **81**, 4347-4352; (c) A. C. Shaikh, D. S. Ranade, S. Thorat, A. Maity, P. P. Kulkarni, R. G. Gonnade, P. Munshi and N. T. Patil, *Chem. Commun.*, 2015, **51**, 16115-16118; (d) D. L. Crossley, I. A. Cade, E. R. Clark, A. Escande, M. J. Humphries, S. M. King, I. Vitorica-Yrezabal, M. J. Ingleson and M. L. Turner, *Chem. Sci.*, 2015, **6**, 5144-5151; (e) D. L. Crossley, J. Cid, L. D. Curless, M. L. Turner and M. J. Ingleson, *Organometallics*, 2015, **34**, 5767-5774; (f) J. S. Lu, S. B. Ko, N. R. Walters, Y. Kang, F. Sauriol and S. Wang, *Angew. Chem.*, 2013, **125**, 4642-4646; *Angew. Chem. Int. Ed.*, 2013, **52**, 4544-4548; (g) Z. J. Zhao, Z. F. Chang, B. R. He, B. Chen, C. M. Deng, P. Lu, H. Y. Qiu and B. Z. Tang, *Chem. Eur. J.*, 2013, **19**, 11512-11517; (h) L. Niu, H. Yang, R. Wang and H. Fu, *Org. Lett.,* 2012, **14**, 2618-2621; (i) H.-L. Wong, W.-T. Wong and V. W.-W. Yam, *Org. Lett.*, 2012, **14**, 1862-1865; (j) N. Ishida, T. Moriya, T. Goya, M. Murakami, *J. Org. Chem.*, 2010, **75**, 8709-8712; (k) S. K. Murphy, C. Baik, J.-S. Lu and S. Wang, *Org. Lett.*, 2010, **12**, 5266-5269; (l) M. Yusuf, K. Liu, F. Guo, R. A. Lalancette, and F. Jäkle, *Dalton Trans.*, 2016, **45**, 4580-4587. (m) H. Amarne, C. Baik, S. K. Murphy and S. Wang, *Chem. Eur. J.*, 2010, **16**, 4750-4761. (n) D. L. Crossley, R. Goh, J. Cid, I. Vitorica-Yrezabal, M. L. Turner and M. J. Ingleson, *Organometallics,* 2017, **36**, 2597-2604. (o) K. Liu, R. A. Lalancette and F. Jäkle, *J. Am. Chem. Soc.,* 2017, **139**, 18170-18173. (p) M. Mamada, G. Tian, H. Nakanotani, J. Su and C. Adachi, *Angew. Chem. Int. Ed.,* 2018, **57**, 12380–12384. (q) A. F. Alahmadi, R. A. Lalancette and F. Jäkle, *Macromol. Rapid Commun.,* 2018, **39**, 1800456.

11 D. L. Crossley, L. Urbano, R. Neumann, S. Bourke, J. Jones, L. A. Dailey, M. Green, M. J. Humphries, S. M. King, M. L. Turner and M. J. Ingleson, *ACS Appl. Mater. Interfaces,* 2017, **9**, 28243−28249.

12 (a) S. B. Ko, J. S. Lu and S. Wang, *Org. Lett.* 2014, **16**, 616-619; (b) D.-T. Yang, Y. Shi, T. Peng and S. Wang, *Organometallics*, 2017, **36**, 2654-2660; (c) M. Stanoppi and A. Lorbach, *Dalton Trans.,* 2018, **47**, 10394–10398. (d) Y.-L. Rao, H. Amarne, J.-S. Lu and S. Wang, *Dalton Trans.*, 2013, **42**, 638-644; (e) Y.-L. Rao

and S. Wang, *Organometallics*, 2011, **30**, 4453-4458; (f) Y.-L. Rao, H. Amarne, S.-B. Zhao, T. M. McCormick, S. Martic, Y. Sun, R.-Y. Wang and S. Wang, *J. Am. Chem. Soc.*, 2008, **130**, 12898-12900; (g) J. Yoshino, N. Kano and T. Kawashima, *Chem. Commun.*, 2007, 559-561. (h) Y.-L. Rao, L. D. Chen, N. J. Mosey and S. Wang, *J. Am. Chem. Soc.*, 2012, **134**, 11026-11034.

13 (a) D. Vagedes, G. Erker, G. Kehr, K. Bergander, O. Kataeva, R. Fröhlich, S. Grimme and C. Mück-Lichtenfeld, *Dalton Trans.*, 2003, 1337-1344; (b) D. Vagedes, G. Kehr, D. König, K. Wedeking, R. Fröhlich, G. Erker, C. Mück-Lichtenfeld and S. Grimme, *Eur. J. Inorg. Chem.*, 2002, **8**, 2015-2021.

14 S. Schraff, Y. Sun and F. Pammer, *J. Mater. Chem. C*, 2017, **5**, 1730–1741.

15 (a) Y. Shi, D. Yang, S. K. Mellerup, N. Wang, T. Peng and S. Wang, *Org. Lett.*, 2016, **18**, 1626-1629; (b) D.-T. Yang, S. K. Mellerup, X. Wang, J.-S. Lu and S. Wang, *Angew. Chem.*, 2015, **127**, 5588-5592; *Angew. Chem. Int. Ed.*, 2015, **54**, 5498-5501;

16 (a) D.-T. Yang, S. K. Mellerup, J.-B. Peng, X. Wang, Q.-S. Li and S. Wang, *J. Am. Chem. Soc.*, 2016, **138**, 11513–11516; (b) S. M. McDonald, S. K. Mellerup, J. Peng, D. Yang, Q.-S. Li and S. Wang, *Chem. Eur. J.*, 2015, **21**, 13961-13970. (c) Y. Shi, X. Wang, N. Wang, T. Peng and S. Wang, *Organometallics*, 2017, **36**, 2677-2684.

17 M. Grandl, Y. Sun, F. Pammer, *Org. Chem. Front.*, 2018, **5**, 336-352.

18 M. Grandl, Y. Sun and F. Pammer, *Chem. Eur. J.*, 2016, **22**, 3976-3980.

19 M. Grandl, B. Rudolf, Y. Sun, D. F. Bechtel, A. J. Pierik and F. Pammer, *Organometallics*, 2017, **36**, 2527–2535.

20 M. Grandl, T. Kaese, A. Krautsieder, Y. Sun and F. Pammer, *Chem. Eur. J.*, 2016, **22**, 14373-14382.

21 M. Grandl and F. Pammer, *Macromol. Chem. Phys.*, 2015, **216**, 2249-2262.

22 M. Grandl, J. Schepper, S. Maity, A. Peukert, E. von Hauff and F. Pammer, *Macromolecules*, 2019, *52*, 1013-1024.

23 B. R. Gragg and G. E. Ryschkewitsch, *Inorg. Chem.*, 1976, **15**, 1201-1205.

24 K. Anton, H. N. H. Pommerenina and H. Nöth, *Chem. Ber.*, 1984, **117**, 2479-2494.

25 H. Nöth and H. Vahrenkamp, *Chem. Ber.*, 1966, **99**, 1049-1067.

26 E. Bernhardt, M. Berkei, H. Willner and M. Z. Schürmann, *Anorg. Allg. Chem.*, 2003, **629**, 677-685.

27 B. Győri, Z. Berente, and I. Lázár, *Polyhedron*, 1998, **6**, 3175-3180.

28 (a) B. Gyori, Z. Berente and I. Lazar, *Polyhedron*, 1998, **17**, 3175-3180. (b) T. Ribbeck, S. H. Zottnick, C. Kerpen, J. Landmann, N. V. Ignat'ev, K. Müller-Buschbaum and M. Finze, *Inorg. Chem.*, 2017, **56**, 2278-2286. (c) J. A. P. Sprenger, J. Landmann, M. Drisch, N. Ignat'ev and M. Finze, *Inorg. Chem.,* 2015, **54**, 3403-3412.

29 (a) J. L. Vidal and G. E. Ryschkewitsch, *Inorg. Chem.*, 1977, **16**, 1673-1677. (b) J. L. Vidal and G. E. Ryschkewitsch, *J. Chem. Soc., Chem. Commun.*, 1976, 192-193.

30 M. Finze, E. Bernhardt, H. Willner and C. W. Lehmann, *J. Am. Chem. Soc.*, 2005, **127**, 10712-10722; K[$(CF_3)_3$BNC]: $\tilde{\nu}$ = 2169 cm^{-1}, K[$(CF_3)_3$BCN]: $\tilde{\nu}$ = 2244 cm^{-1}.

31 M. Finze, E. Bernhardt, H. Willner and C. W. Lehmann, *Organometallics*, **2006**, **25**, 3070-3075.

32 L. Carlton and R. Weber, *Inorg. Chem.,* 1996, **35**, 5843-5850.

33 B. Gyori, J. Emri and I. Feher, *J. Organomet. Chem.*, 1983, **255**, 17-28.

34 M. Joost, G. Alcaraz, L. Vendier, A. Poblador-Bahamonde, E. Clot and S. Sabo-Etienne, *Dalton Trans.*, 2013, **42**, 776-781.

35 (a) M. Hoefler and H. Loewenich, *J. Organometal. Chem.*, 1982, **226**, 229-237. (b) G. Beck, M. F. Lappert and P. B. Hitchcock, *J. Organomet. Chem.*, 1994, **468**, 143-148. (c) A. J. V. Marwitz, S. P. McClintock, L. N. Zakharov and S.-Y. Liu, *Chem. Commun.*, 2010, **46**, 779-781.

36 I. B. Sivaev and V. I. Bregadze, *Coord. Chem. Rev.*, 2014, **270–271**, 75–88.

37 K. Yuan, N. Suzuki, S. K. Mellerup, X. Wang, S. Yamaguchi and S. Wang, *Org. Lett.*, 2016, **18**, 720-723.

38 C. D. Entwistle, A. S. Batsanov, J. A. K. Howard, M. A. Fox and T. B. Marder, *Chem. Commun.*, 2004, 702–703.

39 An isopropyl-group is likely sufficient to enforce >96% α-borylation (see reference 45). However, for preparative expediency *tert*-butylacetylene (bp. = 37-38°C) was used, instead of the even lower boiling isopropylacetylene (bp. = 26.3 °C).

40 The adduct of **1c** with dimesitylborane (Mes_2BH) was incidentally crystallized. ^1H, ^{11}B NMR and crystallographic data have been included in the supporting information.

41 Analogous to the naming of the compounds in the previous section, previously reported ladder boranes derived from 2-(*ortho*-styryl)-pyridine will be referred to by their respective substituents on boron: **BBN**, **BPh_2**, **BPF** (for $B(C_6F_5)_2$).

42 (a) T. B. Marder, P. S. Smith, J. A. K. Howard, M. A. Fox and S. A. Mason, *J. Organometal. Chem.*, 2003, **680**, 165-172. (b) J. Hooz, S. Akiyama, F. J. Cedar, M. J. Bennett and R. M. Tuggle, *J. Am. Chem. Soc.*, 1974, **96**, 274-276. (c) A. Pelter, K. Smith, D. E. Parry and K. D. Jones, *Aust. J. Chem.*, 1992, **45**, 57-70.

43 β-Silicon effect: Stabilizing hyperconjugation between a C-Si σ-bond and p_z-orbitals of carbocation or tricoordinate boron; favors geminal silyl- and boryl-groups.

44 (a) M. A. Brook, *"Silicon in Organic, Organometallic, and Polymer Chemistry"*, John Wiley & Sons, New York, **2000**; b) Z. Rappoport and Y. Apeloig, *"The Chemistry of Organic Silicon Compounds"*, John Wiley & Sons Ltd., Chichester, UK, **2003**.

45 J. A. Soderquist, J. C. Colberg ad L. Del Valle, *J. Am. Chem. Soc.*, 1989, **111**, 4873-4878.

46 (a) D. J. Parks, W. E. Piers and G. P. A. Yap, *Organometallics*, 1998, **17**, 5492-5503; (b) W. E. Piers, D. J. Parks and R. E. von H. Spence, *Angew. Chem.*, 1995, **107**, 895-897; *Angew. Chem. Int. Ed.*, 1995, **34**, 809-811.

47 F. Pammer and F. Jäkle, *Chem. Sci.*, 2012, **3**, 2598-2606**.**

48 (a) Z. Yuan, N. J. Taylor, Y. Sun, T. B. Marder, I. D. Williams and L.-T. Cheng, *J. Organomet. Chem.*, 1993, **449**, 27-37. (b) Z. Yuan, C. D. Entwistle, J. C. Collings, D. Albesa-Jové, A. S. Batsanov, J. A. K. Howard, N. J. Taylor, H. M. Kaiser, D. E. Kaufmann, S.-Y. Poon, W.-Y. Wong, C. Jardin, S. Fathallah, A. Boucekkine, J.-F. Halet and T. B. Marder, *Chem. Eur. J.*, 2006, **12**, 2758-2771.

49 C. D. Entwistle and T. B. Marder, *Chem. Mater.*, 2004, **16**, 4574-4585.

50 H. C. Brown, C. G. Scouten and R. Liotta, *J. Am. Chem. Soc.*, 1979, **101**, 96-99.

51 W. L. F. Armarego and D. D. Perrin, *Purification of Laboratory Chemicals*, 4th Ed. Butterworth-Heinemann, Oxford, 1997.

52 G. R. Fulmer, A. J. M. Miller, N. H. Sherden, H. E. Gottlieb, A. Nudelman, B. M. Stoltz, J. E. Bercaw and K. I. Goldberg, *Organometallics*, 2010, **29**, 2176-2179.

53 N. M. O'Boyle, A. L. Tenderholt and K. M. Langner, *J. Comp. Chem.*, 2008, **29**, 839-845.

54 S. Arndt, M. M. Hansmann, P. Motloch, M. Rudolph, F. Rominger and A. S. K. Hashmi, *Chem. Eur. J.*, 2017, **23**, 2542-2547.

55 X. Cheng, J. Ma, J. Zhi, X. Yang and A. Hu, *Macromolecules*, 2010, **43**, 909–913.

View Article Online
DOI: 10.1039/C9DT01555H